EGFP-FMRP Granules Are Proto-Granules That Can Be Shunted to Stress Granules During a Stress Response

Natalia Dolzhanskaya[1] Wen Xie[1], George Merz[2] and Robert B. Denman[1]*

[1]Department of Molecular Biology and [2]Department of Developmental Neurobiology
New York State Institute for Basic Research in Developmental Disabilities
1050 Forest Hill Road
Staten Island, NY 10314

Short title: EGFP-FMRP forms Proto-Stress Granules

* **Corresponding Author**:
Robert B. Denman, Ph.D.
Head Biochemical Molecular Neurobiology Laboratory
Department of Molecular Biology
New York State Institute for Basic Research in Developmental Disabilities
1050 Forest Hill Road
Staten Island, NY 10314
Tel: (718) 494-5199
Fax: (718) 494-5905
e-mail: rbdenman@yahoo.com

Abbreviations

aDMA, asymmetric dimethylarginine

AdOx, adenosine 2', 3'-dialdehyde

AFPs, autofluorescent proteins

EGFP, enhanced green fluorescence protein

FMRP, fragile X mental retardation protein

FRAP, fluorescence recovery after photobleaching

FXR1P, fragile X related 1 mental retardation protein

GFP, green fluorescent protein

Dcp1a, decapping protein factor 1a

eIF2, eucaryotic initiation factor 2

PRMT, protein arginine methyltransferase

RBP, RNA binding protein

RNA interference, RNA_i

sDMA, symmetric dimethylarginine

TIA1, T-cell internal antigen 1

tM1, tM2, thresholded Manders coefficients

Summary

Overexpressed EGFP-FMRP has been used as a substitute for endogenous fragile X mental retardation protein (FMRP) in protein-protein interaction studies, and in studies concerning the composition, the formation and the localization of neuronal granules. However, the question of whether this tool truly recapitulates the properties of the endogenous protein has not been addressed. Here we demonstrate that overexpressed EGFP-FMRP forms three distinct granule types based on colocalization with various marker proteins. The majority of EGFP-FMRP-containing granules are larger and more amorphous than known granule types. Consistent with this, there is only partial colocalization with stress granule or P-body markers and no colocalization with a putative Drosophila ortholog neuronal granule marker. Nevertheless, agents such as arsenite and hippurstanol, which create endogenous stress granules and P-bodies, drive EGFP-FMRP into such granules. Additionally, whereas inhibiting cellular methyl-protein formation alters the composition of endogenous FMRP-containing stress granules, we found that such treatment had little effect on the formation of EGFP-FMRP granules, or their composition. Altogether these data suggest that many overexpressed EGFP-FMRP granules represent proto-stress granules requiring external stimuli for their conversion. More importantly, the inherent heterogeneity of these granules suggests that caution should be used in extrapolating results obtained with EGFP-tagged surrogates of FMRP to endogenous FMRP granules.

Key words: EGFP, FMRP, stress granules, P-bodies, protein arginine methylation

Introduction

Autofluorescent protein tags (AFPs) have been widely used as tools to study a variety of biological processes including, nervous system development (Brand, 1999), developmental abnormalities (Detrich III, 2008), neural stem cell development (Encinas and Enikolpov, 2008), localization of proteins in specific organelles (Di Giorgi et al., 1999), protein-protein interactions (Kedersha et al., 2005), protein-RNA interactions (Rackham and Brown, 2004), protein (Pierce and Vale, 1999) and mRNA trafficking (Querido and Chartrand, 2008), and membrane dynamics (Lippincott-Schwartz et al., 1999). Green fluorescent protein (GFP) and the myriad of spectral variants comprising the AFPs are relatively small proteins M_r 27, but are much larger than many other widely used tags. As such, it is imperative to demonstrate that the AFP tag does not alter the transport, the localization or the functional properties of the protein being tagged (Lippincott-Schwartz et al., 1999). For example, Ozlu et al used RNA interference (RNA_i) in combination with a TXL-1-GFP fusion to demonstrate that the transgene could functionally replace endogenous TXL-1 at the centrosome (Özlü et al., 2005). On the other hand, there appears to be a significant discrepancy between the localization of endogenous $P58^{TFL}$ with endogenous P-body markers and that of GFP- $P58^{TFL}$ and transfected P-body markers, suggesting that the fusion protein may not adequately mimic the endogenous form (Bloch and Nobre, 2010; Minagawa et al., 2009; Minagawa and Matsui, 2010).

The fragile X mental retardation protein, FMRP, is a RNA binding protein that plays an important role in controlling translation in neurons (Bassell and Warren, 2008). Studies by a number of laboratories have demonstrated that endogenous FMRP associates

with macromolecular granules in the brain, in the neurites of cultured neuronal cells and in the cell bodies of non-neuronal cells (Aschrafi et al., 2005; Didiot et al., 2008; Dolzhanskaya et al., 2006a; Dolzhanskaya et al., 2006b; Kanai et al., 2004; Xie et al., 2009). Immunofluorescence studies have shown that these granules tend to be small and not that prevalent. In contrast, AFP-tagged FMRPs have been used by a number of laboratories to assess various questions concerning neuronal granule make up and dynamics (Antar et al., 2005; Barbee et al., 2006; Castren et al., 2001; Cziko et al., 2009; Darnell et al., 2005; De Diego Otero et al., 2002; Dictenberg et al., 2008; Levenga et al., 2009; Ling et al., 2004; Pfeiffer and Huber, 2007). These granules tend to be much larger than endogenous FMRP granules and also much more prevalent in dendrites. However, the question of what type(s) of granules AFP-FMRP represents has not been adequately addressed.

Here we have examined EGFP-FMRP expression in HeLa cells using a variety of known granule marker proteins and under various conditions known to induce the formation of specific granule types or modulate their composition. Our studies demonstrate that EGFP-FMRP granules fall into at least three different functional classes, the majority of which appears to be a proto-stress granule. The implications of these results are discussed.

Results

EGFP-FMRP expression results in a heterogeneous array of granules

Fluorescence microscopy of primary hippocampal neurons and Neuro 2A cells transfected with a plasmid encoding an EGFP-FMRP fusion protein has shown that its expression was in the form of granules that were confined largely to the cytoplasm (Antar

et al., 2004; Darnell et al., 2005; Pfeiffer and Huber, 2007). Here we show that HeLa cells transfected with the same plasmid express fluorescent granules with an assortment of sizes. In contrast, transfection of the parent vector shows that EGFP exhibits diffuse, non-granular cytoplasmic expression, Fig. 1A. Analysis of the distribution of EGFP-FMRP granules reveals that they fall into three different size categories (small, intermediate and large), Fig. 1B. In contrast, endogenous FMRP granules were much more homogeneous and mainly correspond in size to the smaller size EGFP-FMRP granules, Fig. 1C. These data are consistent with two competing hypotheses. One possibility is that individual EGFP-FMRP granules have disparate compositions and possibly differing functions. The other likelihood is that the population of EGFP-FMRP granules represents nascent core particles of the same composition, but with differing aggregation states.

EGFP-FMRP expression and stress granule markers

Previous studies have shown that endogenous FMRP forms a variety of granule types including stress granules. Stress granules can be formed in response to heat shock (Mazroui et al., 2002), oxidative stress (Thomas et al., 2004), RNA binding protein over expression (Solomon et al., 2007), expression of a phosphomimetic mutant form of eukaryotic initiation factor 2 (eIF-2) (McEwen et al., 2005) and interfering with eIF4A activity (Mazroui et al., 2006). To determine whether the granules formed by expression of EGFP-FMRP were stress granules, rat pheochromocytoma cells (PC12) were transiently transfected with an EGFP-FMRP expression vector. Twenty four hours later the cells were immunostained with anti-TIA1, an RNA binding protein which detects core stress granules (Kedersha et al., 2005), and then visualized by confocal microscopy.

As shown in Fig. 2 (panel a), punctate EGFP-FMRP expression was observed in the cytoplasm of PC12 cells. In contrast, but as expected, TIA1 was found in both the cytoplasm and the nucleus, Fig. 2 (panel b). In the cytoplasm TIA1 and EGFP-FMRP co-localized in large perinuclear granules; however, there were a host of smaller EGFP-FMRP granules that did not contain TIA1. This general pattern of incomplete co-localization was also observed in HeLa cells expressing EGFP-FMRP, Fig. 2 (panels d-i). Nevertheless, it did not appear that granule size was a determining factor in the co-localization of TIA1 and EGFP-FMRP, rather there appeared to be cells with extensive co-localization, and cells with poor co-localization (compare panels d-f with g-i). However, overall cells exhibiting colocalization were in the minority (see below). Interestingly, in the latter cells, TIA1 was largely found in the nucleus.

To quantify the extent of colocalization between EGFP-FMRP and TIA1 we performed colocalization analyses. By manually masking nuclear staining and setting threshold limits on each fluorescence channel we were able to differentiate granular versus non-granular staining. Table 1 shows the thresholded Manders coefficients tM1 (fraction of red in the green channel) and tM2 (fraction of green in the red channel) for the EGFP-FMRP granules under different conditions. In the absence of treatment the majority of EGFP-FMRP granules were devoid of TIA1; however, following treatment with either sodium arsenite or hippurstanol there was a significant shift of TIA1 into these granules.

We next examined colocalization between EGFP-FMRP granules and another stress granule marker, FXR1P. Endogenous FXR1P extensively colocalizes with endogenous FMRP in arsenite induced stress granules (Dolzhanskaya et al., 2006a;

Dolzhanskaya et al., 2006b), Fig. 3A (panel c). However, as shown in Fig. 3B (panels d-f), colocalization between EGFP-FMRP granules and FXR1P was also incomplete. Again however, in the presence of arsenite EGFP-FMRP granules almost completely colocalized with FXR1P, Fig. 3C (panel i).

Do EGFP-FMRP granules contain phospho-eIF2?

There are two distinct mechanisms that initiate stress granule formation, both of which involve blocking translational initiation. Environmental stresses such as heat shock, osmotic shock and oxidative stress produce stress granules via phosphorylation of eukaryotic initiation factor 2α (p-eIF2α) (Kedersha et al., 2007; Lu et al., 2001). On the other hand, stress granules can also be induced *via* an eIF2α-independent pathway by blocking cap-dependent initiation during poliovirus infection (Mazroui et al., 2006; White et al., 2007). As phosphorylated eIF2α can associate with stress granules (Kimball et al., 2003), we next determined whether EGFP-FMRP granules contained phosphorylated eIF2α; the results are shown in Fig. 4A. Phospho-eIF2α was weakly and diffusely localized within the cytoplasm of HeLa cells. Significantly, the staining intensity of both EGFP-FMRP expressing cells and non-expressing cells were equivalent, implying that the expression of EGFP-FMRP does not markedly increase phospho-eIF2α expression. Consistent with this there is little colocalization with EGFP-FMRP granules, Fig. 4A (panel c). In contrast, arsenite-induced TIA1-containing stress granules did exhibit some colocalization with phospho-eIF2α; however, the phospho-eIF2α-granules were much smaller than the TIA1-stress granules, Fig. 4B (panel f), indicating that they were associated with the granules rather than core constituents.

Hippuristanol a natural product derived from *Isis hippuris* inhibits eIF4A, and by doing so induces stress granule formation (Lindqvist et al., 2008). We next determined the effect hippuristanol had on EGFP-FMRP granule formation. As shown in Fig. 5A (panel b) hippuristanol induced a robust formation of TIA1-containing stress granules in both EGFP-FMRP-expressing cells and in EGFP-FMRP-nonexpressing cells. In EGFP-FMRP-expressing cells, TIA1 and EGFP-FMRP colocalized extensively Fig. 5A (panel c) and Table 1. In contrast, we observed no colocalization with phospho-eIF2α; Fig. 5A (panels d-f).

In the absence of hippuristanol, EGFP-FMRP-nonexpressing cells exhibited few TIA1 granules, whereas EGFP-FMRP-expressing cells more often exhibited colocalizing TIA1 granules, Fig. 5B (panel i). However, as with the experiments shown in Fig. 2, there were also many instances of EGFP-FMRP-expressing cells that were devoid of TIA1 granules, Table 1. In addition, phospho-eIF2α and EGFP-FMRP did not colocalize in the absence of hippurstanol, Fig. 5B (panel l).

EGFP-FMRP granules and the P-body marker Dcp1a

P-bodies are another type of granule, distinct from, but associated with stress granules (Anderson and Kedersha, 2006). Studies have shown that certain proteins shuttle between stress granules and P-bodies, while others do not, marking them as core constituents (Kedersha et al., 2005). The decapping factor, Dcp1a, is a core constituent of P-bodies (Cougot et al., 2004). To determine whether EGFP-FMRP was associated with P-bodies HeLa cells were transiently transfected with an EGFP-FMRP expression vector. Twenty four hours later the cells were immunostained with anti-Dcp1a and visualized by confocal microscopy. Fig. 6A (panel c) shows that EGFP-FMRP granules

can occasionally overlap with Dcp1a-containing granules, indicating that a portion of EGFP-FMRP is present in P-bodies. Quantitative colocalization analyses reveal however, that like the stress granule markers, the extent of colocalization is very weak, Table 1. Treating cells with sodium arsenite for 20 min following transfection produces stress granules and P-bodies (Kedersha et al., 2007). Under these conditions Dcp1a granules associate more closely with EGFP-FMRP granules, although they generally do not overlap, Fig. 6B (panel f) and Table 1. In this respect, Dcp1a mimics Hsp70c, Fig. 6C (panel l).

Thus, exogenously expressed EGFP-FMRP sorts into at least three granule types: stress granules, P-bodies and a unique granule, which represents the largest fraction of this set.

The physical characteristics of EGFP-FMRP granules differ from stress granules and P-bodies

To further characterize EGFP-FMRP granules we undertook morphometric analyses of two readily quantifiable features, granule shape and granule size. The results were compared to arsenite-induced TIA1 granules, hippuristanol-induced TIA1 granules and endogenous Dcp1a-containing P-bodies. As expected, we found that the Dcp1a-containing P-bodies were significantly smaller than arsenite-induced stress granules hippuristanol-induced stress granules, and EGFP-FMRP granules. On the other hand, EGFP-FMRP granules were both substantially larger and more amorphous than the other granules, Table 2. These data again highlight differences between EGFP-FMRP granules and other granule types.

The dynamic properties of EGFP-FMRP granules mimic stress granules

Emetine inhibits protein synthesis elongation (Gay et al., 1989; Grollman and Huang, 1976; Yamasaki et al., 2007) altering the dynamic equilibrium between polyribosomes and stress granules. Kedesha *et al* found that in DU-145 cells treated with arsenite the addition of emetine at concentrations that inhibit protein synthesis effectively "dissolved" TIA1-containing stress granules (Kedersha et al., 2000). Therefore, we used emetine to assess the dynamic interrelationship between EGFP-FMRP-containing granules and polyribosomes. We first demonstrated that endogenous TIA1 stress granules and endogenous FMRP stress granules in HeLa cells treated with arsenite are substantially altered by emetine, Fig. 7A. Specifically, the sizes of the granules in the emetine-treated cells were much smaller than the arsenite-induced stress granules, Fig. 7B-C. We then applied this paradigm to assess the effect of emetine on EGFP-FMRP granules. Here we found that both untreated EGFP-FMRP granules and arsenite-treated EGFP-FMRP granules responded to emetine in much the same way as TIA1 and FMRP stress granules, Fig. 8A-C.

Fluorescence recovery after photobleaching is a method that is often used to characterize the dynamic properties of granules (Kedersha et al., 2005; Kedersha et al., 2008). For example, Antar *et al* examined the effect nocodazole had on EGFP-FMRP granules in cultured hippocampal neurons (Antar et al., 2005) and found their transport within dendrites was microtubule-dependent. Here we performed similar analyses on EGFP-FMRP granules comparing them to ones formed following arsenite treatment. In the absence of treatment EGFP-FMRP granules exhibited a range of motilities. Some granules were quite stationary, while others were highly mobile. FRAP analysis of these granules in the absence of treatment revealed they recovered 50% of their unbleached

intensity within 10 minutes, implying that there is a dynamic exchange between non-granular EGFP-FMRP and the granules, Fig. 9A-C. To determine whether conditions that induce the formation of stress granules alters the recovery of EGFP-FMRP granules, HeLa cells were treated with arsenite and FRAP was performed on the resulting perinuclear granules. The results showed that the treatment increased the rate of recovery slightly, but not significantly, Fig. 9D.

EGFP-FMRP granules contain methylated proteins, but do not require methylated proteins for their formation

Previously we showed that endogenous FMRP-containing stress granules contain asymmetric dimethylarginine-modified proteins (aDMA-proteins) and that the cell's methylation state affected their composition (Dolzhanskaya et al., 2006a). To examine the effect inhibiting cellular protein methylation had on the formation and distribution of EGFP-FMRP granules, HeLa cells transiently expressing EGFP-FMRP were treated for twenty four hours with the general methylation inhibitor adenosine 2', 3'-dialdehyde (AdOx). Subsequently, the cells were immunostained with anti-TIA1 and visualized by confocal microscopy. As was the case in the untreated cells (Fig. 2) there appeared to be EGFP-FMRP-expressing cells that had extensive colocalization with TIA1 and cells that had relatively little colocalization. Therefore, the cell's protein methylation state appears to have little effect upon the interaction of EGFP-FMRP and TIA1.

We next examined whether EGFP-FMRP granules contained asymmetrically dimethylated (aDMA) proteins. HeLa cells, transiently expressing EGFP-FMRP were incubated in the absence or presence of AdOx for twenty-four hours (as above). Subsequently, the cells were immunostained with two antibodies that detect different sets

of aDMA proteins. For the untreated cells, cytoplasmic EGFP-FMRP granules exhibited extensive colocalization with the proteins detected by these two antibodies, Fig. 10A (panels a-c and f-h). Importantly, AdOx treatment resulted a marked reduction in immunoreactivity, both overall and in the granules, Fig. 10A (panels c-e and i-k), indicating that the staining was indeed due to aDMA proteins. Quantitative analyses showed that under the conditions used the extent of the reduction was ca. 50 %, Fig. 10B.

The above data suggested that reduced methylation of endogenous proteins does not drastically alter the composition of EGFP-FMRP granules; however, it does not inform one as to whether asymmetric dimethylation affects the formation of EGFP-FMRP granules. To address this question, HeLa cells were pre-treated with AdOx for twenty-four hours prior to transfection. Subsequently, the cells were transfected with the EGFP-FMRP expression vector in AdOx-containing media. As shown in Fig. 11A, EGFP-FMRP granules were readily detected even in the continued presence of AdOx implying that full protein methylation is not required for the formation of these granules. In concert with these data treatment with AdOx had no effect on the distribution of EGFP-FMRP granules, Fig. 11B.

We next assessed whether EGFP-FMRP granules contained symmetrically dimethylated (sDMA) proteins. In the absence of treatment we found that the symmetrically dimethylated protein immunoreactivity localized primarily to the nucleus, Fig. 12A (panel b). Notably, the cytoplasmic staining partially associated with EGFP-FMRP granules, indicating that these granules are heterogeneous with respect to sDMA-containing proteins. However, treating the cells with arsenite following transfection resulted in the recruitment of a significant amount of sDMA proteins into cytoplasmic

granules, and in EGFP-FMRP expressing cells; almost all of the EGFP-FMRP granules contained sDMA-modified proteins, Fig. 12A (panels g-i). Treating the cells with AdOx prior to arsenite treatment significantly decreased the sDMA protein immunoreactivity (Fig. 12A panel k and Fig. 10B) although the extent of colocalization with EGFP-FMRP granules was unchanged, Fig. 12B.

Consistent with the immunostaining results, Western blot analyses showed that AdOx treatment decreased the amount of aDMA and sDMA in various proteins, albeit to different extents. In contrast, the expression of five different protein arginine methyltransferases (PRMTs) was unaffected by treatment with AdOx, Fig. 13.

As these data unequivocally demonstrate sDMA is harbored in arsenite-treated EGFP-FMRP granules we next endeavored to ascertain whether endogenous stress granules also contained sDMA-modified proteins. To this end we treated HeLa cells with arsenite and then immunostained them with antibodies to TIA1 and sDMA. We observed significant colocalization between sDMA-modified proteins and TIA1-containing stress granules, Fig. 14.

Identities of sDMA-modified proteins in Stress Granules

Anti-SYM10 is a well-characterized antibody, which primarily detects proteins associated directly or indirectly with pre-mRNA splicing (Boisvert et al., 2003a). In particular, the Sm proteins (SmB/B', SmD1/D3, and U6 small nuclear RNA-associated Sm-like proteins Lsm4 and Lsm8) have been shown to contain symmetric dimethylarginine (Brahms et al., 2001) and are known epitopes for SYM10 (Boisvert et al., 2002). Cziko *et al* have shown that the *smD3* gene dominantly suppresses the *sev-dfmr1* rough-eye phenotype, and the encoded protein, SmD3, partially co-localizes with

YFP-dFmr1 in larval ventral ganglion cell neuronal granules (Cziko et al., 2009). Therefore, it was of interest to determine whether EGFP-FMRP or endogenous FMRP colocalized with human SmD3. We found, in contrast to the heterologous YFP-dFmr1 variant that human SmD3 did not colocalize with endogenous FMRP granules, FMRP arsenite-induced stress granules, TIA1 arsenite-induced stress granules, or with EGFP-FMRP granules, Fig. 15A-C, nor did they colocalize with another Sm subtype, SmB/B', Fig. 16.

PRMT3 localizes to Stress Granules

The localization of both aDMA-modified proteins and sDMA-modified proteins in stress granules led us to wonder whether any of the PRMTs also colocalize with these granules and potentially control their composition. Because of its known association with ribosomes (Swiercz et al., 2007), we were particularly attracted by the possibility PRMT3 might be found in stress granules. Therefore, we measured the subcellular distribution of PRMT3 in the presence and absence of arsenite treatment by confocal immunofluorescence microscopy using endogenous FXR1P as a stress granule marker. We found that in the presence of arsenite PRMT3 was found in perinuclear cytoplasmic granules that colocalized with FXR1P stress granules, Fig. 17. Interestingly, pre-treatment of the cells with AdOx resulted in the relocation of most of PRMT3 to the nucleus, effectively eliminating the colocalization. (The basis of this effect is currently unknown). In contrast, we found that neither class II PRMT (PRMT5 nor PRMT7) colocalized with TIA1-containing stress granules.

Discussion

Heterologously expressed EGFP-FMRP has been used as a surrogate marker for endogenous FMRP by several laboratories in a wide variety of studies (Antar et al., 2005; Castren et al., 2001; Cougot et al., 2008; Darnell et al., 2005; Davidovic et al., 2004; De Diego Otero et al., 2002; Dictenberg et al., 2008; Levenga et al., 2009; Pfeiffer and Huber, 2007). Like endogenous FMRP, EGFP-FMRP was found to co-sediment with polyribosomes in cultured neurons (Darnell et al., 2005). Additionally, Antar *et al* showed that EGFP-FMRP was transported to dendrites in the form of granules (Antar et al., 2004). Subsequent work showed that these granules associated with mRNA and kinesin transport motors (Wang et al., 2008) and were responsive to stimulation by the mGluR agonist DHPG. These too are properties of endogenous FMRP (Hou et al., 2006; Kanai et al., 2004).

However, important questions regarding EGFP-FMRP remained to be addressed. Were these granules uniformly composed? Did they correspond to one or more types of known granules? Could they be modified by various treatments that are known to affect the formation and/or composition of known granule types? Answering these questions in light of the well-established properties of endogenous FMRP granules (Didiot et al., 2008; Dolzhanskaya et al., 2006a; Dolzhanskaya et al., 2006b) was one of the objectives of this study.

In contradistinction to endogenous FMRP granules, which are small, and while pervasive in cultured cells not particularly prevalent, (Cougot et al., 2008; Dolzhanskaya et al., 2006a; Dolzhanskaya et al., 2006b) EGFP-FMRP granules are large, and amorphous. In fact, they tend to be larger and more non-uniformly round than stress granules, Table 2. Underlying this size/shape heterogeneity we found that EGFP-FMRP

granules also are non-uniformly composed. Endogenous FMRP absent environmental stress does not colocalize with stress granule markers; however, in the presence of a stressor such as heat or arsenite FMRP is recruited into stress granules (Didiot et al., 2008; Dolzhanskaya et al., 2006a; Mazroui et al., 2002). Using well-known stress granule markers (TIA1 and FXR1P) we found that EGFP-FMRP granules weakly colocalize with these proteins in the absence of a bonafide stressor; however, stressing EGFP-FMRP-expressing cells with either arsenite or hippurstanol resulted in a marked increase in colocalization, Figs 2, 3 and Table 1. Thus, native EGFP-FMRP granules are composed of at least two granule types existing in dynamic equilibrium with each other.

Contradicting data exists regarding the association of FMRP with P-bodies. Several lines of evidence have shown that FMRP, or its Drosophila counterpart dFMR1, interact specifically with components that are associated with P-bodies (Anderson and Kedersha, 2006). Ishizuka et al first demonstrated that dFMR1 interacted with Ago2 and the RNA helicase Dmp68 (Ishizuka et al., 2002); more recently Cheever et al showed that FMRP interacts with Dicer in a phosphorylation-dependent fashion (Cheever and Ceman, 2009). Moreover, immunofluorescence studies of rat dorsal root ganglia cultures (DRG) showed that endogenous FMRP partially overlapped the staining of both Ago3 and Ago4 in rat dorsal root ganglion processes (Hengst et al., 2006), while Cougot et al and Barbee et al demonstrated that EGFP-FMRP and GFP-dFMR1 colocalized with Dcp1 (Barbee et al., 2006; Cougot et al., 2008). Nevertheless, Didiot et al failed to observe much localization of endogenous FMRP with Dcp1a in HeLa cells (Didiot et al., 2008). Here we found a weak colocalization between EGFP-FMRP granules and the P-body marker Dcp1a, Fig. 6 and Table 1. We hypothesize that the differing results may be related to

differences in the species and tissue expression of P-body components (González-González et al., 2008).

As there are several stressors that trigger the formation of stress granules, so too there are at least two independent mechanisms by which they form. Arsenite treatment induces the phosphorylation of eucaryotic initiation factor 2α, eIF2α, which sequesters a ternary complex between itself, initiator Met-tRNA and GTP. This, in turn, results in the recruitment of the T-cell internal antigen (TIA-1), into 48S* pre-initiation complexes, which are then no longer competent to form 80S monosomes. Hippurstanol, on the other hand, inhibits eIF4A without affecting eIF2α phosphorylation (Mazroui et al., 2006). We found in both arsenite-treated and hippurstanol-treated cells that there was little association between phospho-eIF2α and EGFP-FMRP granules; however, arsenite-induced TIA1-containing stress granules showed a modest colocalization consistent with data from other laboratories (Kedersha et al., 2002; Kimball et al., 2003). Again, these data underscore fundamental differences between EGFP-FMRP granules and stress granules.

We also determined whether EGFP-FMRP granules were in dynamic equilibrium with polyribosomes and/or the pool of non-granular cytoplasmic EGFP-FMRP by emetine treatment (Kedersha et al., 2000) and FRAP (Lippincott-Schwartz et al., 1999), respectively. Here we found that EGFP-FMRP granules mimic the properties of endogenous FMRP, implying that there are certain "core characteristics" of granules that are invariant (Buchan and Parker, 2009).

Like a host of other post-translational modifications (Kwon et al., 2007; Mazroui et al., 2007; Wasserman et al., 2009), protein methylation regulates stress granules. In

particular, we have previously demonstrated that pharmacological inhibition of protein methylation altered the FXR1P content of FMRP-containing stress granules (Dolzhanskaya et al., 2006a). Thus, it was of interest to determine the role methylation played in EGFP-FMRP granule formation. We found, in contrast to endogenous FMRP, that EGFP-FMRP granules harbored aDMA-containing proteins, but that the modification of these proteins was not required for granule formation, Figs 10-11. We also showed that the sDMA content of EGFP-FMRP granules was heterogeneous. Nevertheless, following arsenite treatment sDMA-containing proteins were recruited into endogenous stress granules and EGFP-FMRP stress granules, Fig. 12.

The sDMA antibody that was used in this study was raised to the peptide $R^{sDMA}GR^{sDMA}GR^{sDMA}GR^{sDMA}G$ and was previously shown to preferentially recognize sDMA-containing proteins (Boisvert et al., 2002). In fact, Boisvert *et al* detected more than 29 potential sDMA-containing proteins in immunoprecipitation reactions using this antibody (Boisvert et al., 2003b). Among the proteins identified in this screen and subsequently confirmed as harboring sDMA was the splicing-related protein SmD3. As Cziko *et al* recently determined that GFP-dFmr1 neuronal granules partially colocalized with YFP-SmD3 (Cziko et al., 2009), it was of significant interest to determine whether human endogenous SmD3 (hSmD3) colocalized with EGFP-FMRP- or endogenous FMRP granules. We found that hSmD3 failed to colocalize with endogenous FMRP or with EGFP-FMRP granules in the presence or the absence of stress, nor did it colocalize with TIA-containing stress granules, Fig. 15. These results agree with the findings of Zhang *et al* who demonstrated that the neurites of mouse primary motor neurons were deficient in endogenous Sm proteins although they contained significant amounts of

SMN granules (Zhang et al., 2006). Subsequent work by Piazzon *et al* has shown that FMRP-containing SMN complexes are also devoid of Sm proteins (Piazzon et al., 2007). More importantly however, the data underscore the potential difficulties of using over expressed AFP-proteins as markers of endogenous proteins and of extrapolating results of protein ortholog studies.

The localization of both sDMA-modified proteins and aDMA-modified proteins in stress granules led us to wonder whether any of the PRMTs also colocalize with these granules and potentially control their composition. Precedence for this can be found in the fact that many PRMTs act in complexes to regulate transcription (Chen et al., 2002). More importantly, post-translational regulation of stress granules is emerging as an important, albeit little understood feature of the stress response. Besides the effects the methylation inhibitor AdOx has on stress granule composition, recent work has shown that phosphorylation (Wasserman et al., 2009), acetylation (Kwon et al., 2007) and ubiquitination (Kwon et al., 2007; Mazroui et al., 2007) regulate stress granule dynamics *via* direct incorporation of the modifying enzymes. Furthermore, it is known that PRMT3 uniquely associates with ribosomes and methylates ribosomal protein S2 (Swiercz et al., 2004), and the small subunit of the ribosome is a core constituent of stress granules. Thus, we were particularly attracted by the possibility PRMT3 might be found in stress granules. Our findings are consistent with an association of PRMT3, but not PRMT5 and PRMT7 in stress granules, Fig. 17, although the ramifications of this observation remain to be fleshed out.

Overall, our work has shown both similarities and marked differences between endogenous FMRP granules and heterologous EGFP-FMRP granules. The similarities in

the various RNA binding proteins (RBPs) and translational components that are associated with endogenous and heterologous granules highlight the fact that granules of a particular class (*e.g.* stress granules) share a common core that is either added to or subtracted from to construct a granule of unique composition and function. The differences between endogenous FMRP granules and heterologous EGFP-FMRP granules, particularly the class heterogeneity of the EGFP-FMRP granules and the fact that exogenous treatment can alter the compositional balance of the granule class (*e.g.* stress granule *vs.* non-stress granule), point to the inter-convertibility of these granules. Additionally, differences in the post-translational modification state of EGFP-FMRP granules and FMRP granules suggest that they may be uniquely regulated. Thus, the post-translational, compositional and functional heterogeneity of FMRP granules (and probably all granules) pose tremendous challenges in our ability to understand the biochemistry and dynamics of their formation and of their modulation.

Materials and Methods

Reagents

Sodium arsenite, adenosine 2', 3'-dialdehyde (AdOx) and emetine were purchased from Sigma. Hippurstanol was a kind gift from Jerry Pelletier (McGill Cancer Center, McGill University, Montreal, Quebec, Canada).

Plasmids and Transfection

A mammalian expression plasmid containing an enhanced green fluorescent-FMRP fusion protein under the control of a cytomegalovirus promoter pEGFP-FMRP (Antar et al., 2004) was a kind gift of Dr. Gary Bassell (Emory University, Atlanta, GA).

The parent vector, pEGFP-C2, was purchased from Clontech. Cells (3×10^5/35 mm dish) were transfected with 1 μg of plasmid DNA using Lipofectamine Plus (Invitrogen).

Proteins and antibodies

FMRP mAb-2160, which recognizes an epitope in the N-terminus of human FMRP, and normal mouse serum were purchased from Chemicon. Phospho-eIF2α pAb (Ser52) (KAP-CP131) and Hsp70c mAb (HSP-820) were obtained from StressGen. TIA1 pAb (sc-1751), FXR1P pAb (sc-10552) and SmB/B'/N pAb (sc-25372) were purchased from Santa Cruz. Asymmetric dimethylarginine pAb (ASYM24) and symmetric dimethylarginine pAb (SYM10) were purchased from Millipore. Dimethylarginine pAb (mRG) was obtained from CH3 Biosystems. Protein arginine methyltransferase antibody, PRMT1 was obtained from Abcam (ab70724), while PRMT3 pAb (07-256), PRMT4 pAb (AB3345), PRMT5 pAb (07-405) and PRMT7 pAb (07-639) were obtained from Millipore. SmD3 antibody (HPA001170) was purchased from Sigma. hDcp1a pAb was a kind gift of J. Lykke-Andersen (University of Colorado, Boulder, CO).

Cell culture

HeLa cells were grown at 37°C in 5% CO_2 and maintained in DMEM supplemented with 10% FBS, 100 U/ml penicillin and 100 μg/ml streptomycin. In some cases, the cells were treated with 20 μM AdOx, 0.5 mM sodium arsenite, 10 μM hippurstanol, or with 10 μg/ml emetine and processed as indicated (Dolzhanskaya et al., 2006a).

PC12 cells were grown at 37 °C in 5% CO_2 and maintained in DMEM supplemented with 10% FBS and 200 mM glutamine, 100 U/ml penicillin and 100 μg/ml

streptomycin. In some cases, the cells were treated with 20 μM AdOx or with 0.5 mM sodium arsenite and harvested as indicated (Dolzhanskaya et al., 2006b).

Gene expression in cultured cells

Western blotting was carried out according to protocols set forth by the manufacturer for each antibody or as previously described (Dolzhanskaya et al., 2006a). For immunostaining, cells were grown on poly-L-lysine coated coverslips in the presence or absence of 20 μM AdOx and in the presence or absence of 0.5 mM sodium arsenite as indicated. The cells were fixed in 2% paraformaldehyde for 10 minutes and washed with PBS and then blocked in (RPMI1640 base medium, 0.05 % saponin, 0.1 % sodium azide, 2 % goat serum) for 30 minutes at room temperature. Subsequently, the cells were stained with antibodies to FMRP (1:500), TIA-1 (1:100), Hsp70 (1:300), FXR1P (1:50), hDcp1 (1:200), phospho-eIF2α (1:100), ASYM24 (1:100), mRG (1:150), SmD3 (1:75) SmB/B'/N (1:50) or SYM10 (1:100) for 1 hour. This was followed by incubation with Alexa Fluor secondary antibodies (1:500 dilution) for 30 minutes at room temperature. Finally, the coverslips were washed in RPMI1640 base medium, 1 % goat serum and mounted in buffered glycerol. Fluorescence was detected with an Eclipse 90i dual laser-scanning confocal microscope (NIKON). Images were acquired at 20-100x magnification.

Image analyses

Relative EGFP-FMRP granule size (pixels^2) was determined from select confocal images. Granules in each image file were defined using the threshold function in Image J (http://rsb.info.nih.gov.80/ij/). Granule areas were then calculated using the Analyze Particles feature. For calculations all images were taken at 40x magnification and the

entire image was quantified; thereby ensuring a uniform pixel size. The circularity of the granules, 4π (area/perimeter^2), was calculated similarly. The data were then imported into Excel for subsequent analysis. For presentation, granule size distributions were all normalized to 500 particles and the normalized distributions were compared using the F-test for two sample variance. Protein co-localization measurements were performed by counting single- and double-stained granules of acquired images (Thomas et al., 2004). Co-localization was determined using the JaCoP Plugin (Bolte and Cordelieres, 2006; Didiot et al., 2008). Line scans of the cellular fluorescence intensity (Biron et al., 2004) were also acquired using Image J software.

FRAP

Fluorescence recovery after photobleaching (FRAP) was measured as described by Wang *et al* with modification (Wang et al., 2008). HeLa cells were cultured on 40 mm coverslips and transfected with pEGFP–FMRP. Twenty four hours the cells were mounted in Sykes-Moore chambers (Bellco Glass Inc., Vineland, NJ) on a Nikon 90i microscope coupled to a Nikon C1 three-laser scanning confocal system (NIKON Instruments Inc., Melville, NY). The cells were maintained at 37 C with an air curtain incubator (NevTek, Williamsville, Va). Baseline images of EGFP-FMRP-expressing cells were acquired and select regions of interest (ROI) within the transfected cells were bleached to 10 % or less of their initial intensity with the argon laser. Time-lapse images of the recovery were obtained at 30 second intervals. Image data before and after bleaching was first concatenated and then converted into animated GIF files and processed using Image J software. The mean fluorescence within select bleached and control ROI was obtained using the Analyze Particles function, while fluorescence of

particular EGFP–FMRP granules was measured using the linescan feature. Data were exported into Microsoft Excel for subsequent analysis. In some cases, cells were treated with arsenite 0.5 mM for 2 minutes prior to bleaching to induce stress granules. Arsenite was maintained throughout the 20 minute FRAP time-lapse. A total of five arsenite-treated cells and five untreated cells were examined.

Acknowledgements

We thank Drs. Ying-Ju Sung and W. Ted Brown for helpful discussions concerning this manuscript. These studies were generously supported by the New York State Research Foundation for Mental Hygiene and the FRAXA Research Foundation.

References

Anderson, P. and Kedersha, N. (2006). RNA granules. *J. Cell Biol.* **172**, 803-808.

Antar, L. N., Afroz, R., Dictenberg, J. B., Carroll, R. C. and Bassell, G. J. (2004). Metabotropic glutamate receptor activation regulates fragile X mental retardation protein and Fmr1 mRNA localization differentially in dendrites and at synapses. *J. Neurosci.* **24**, 2648-2655.

Antar, L. N., Dictenberg, J. B., Plociniak, M., Afroz, R. and Bassell, G. J. (2005). Localization of FMRP-associated mRNA granules and requirement of microtubules for activity-dependent trafficking in hippocampal neurons. *Genes Brain Behavior* **4**, 350-359.

Aschrafi, A., Cunningham, B. A., Edelman, G. M. and Vanderklish, P. W. (2005). The fragile X mental retardation protein and group I metabotropic glutamate receptors regulate levels of mRNA granules in brain. *Proc Nat'l Acad Sci* **102**, 2180-2185.

Barbee, S. A., Estes, P. S., Cziko, A.-M., Hillebrand, J., Luedeman, R. A., Coller, J. M., Johnson, N., Howlett, I. C., Geng, C. and Ueda, R. (2006). Staufen- and FMRP-containing neuronal RNPs are structurally and functionally related to somatic P bodies. *Neuron* **52**, 997-1009.

Bassell, G. J. and Warren, S. T. (2008). Fragile X syndrome: Loss of local mRNA regulation alters synaptic development and function. **60**, 201-214.

Biron, V. L., McManus, K. J., Hu, N., Hendzel, M. J. and Underhill, D. A. (2004). Distinct dynamics and distribution of histone methyl-lysine derivatives in mouse development. *Developmental Biology* **276**, 337-351.

Bloch, D. B. and Nobre, R. (2010). p58TFL does not localize to messenger RNA processing bodies - Letter. *Molecular Cancer Research* **8**, 131-132.

Boisvert, F.-M., Cote, J., Boulanger, M.-C. and ;Richard, S. (2003a). A proteomic analysis of arginine methylated protein complexes. *Mol Cell Proteomics* **2**, 1319-1330.

Boisvert, F.-M., Cote, J., Boulanger, M.-C., Cleroux, P., Bachand, F., Autexier, C. and Richard, S. (2002). Symmetrical dimethylarginine methylation is required for the localization of SMN in Cajal bodies and pre-mRNA splicing. *J. Cell Biol.* **159**, 957-969.

Boisvert, F.-M., Cote, J., Boulanger, M.-C. and Richard, S. (2003b). A proteomic analysis of methylated protein complexes. *Mol & Cell Proteomics* **2**, 1319-1330.

Bolte, S. and Cordelieres, F. P. (2006). A guided tour into subcellular colocalization analysis in light microscopy. *Journal of Microscopy* **224**, 213-232.

Brahms, H., Meheus, L., de Brabandere, V., Fischer, U. and Luhrmann, R. (2001). Symmetrical dimethylation of arginine residues in spliceosomal Sm protein B/B' and the Sm-like protein LSm4, and their interaction with the SMN protein. *RNA* **7**, 1531-1542.

Brand, A. (1999). GFP as a cell and developmental marker in the Drosophila nervous system. In *Green Fluroescent Proteins*, vol. 58 (eds K. F. Sullivan and S. A. Kay), pp. 165-180. San Diego: Academic Press.

Buchan, J. R. and Parker, R. (2009). Eukaryotic stress granules: the ins and outs of translation. *Mol Cell* **36**, 932-941.

Castren, M., Haapasalo, A., Oostra, B. and Castren, E. (2001). Subcellular localization of fragile X mental retardation protein with the I304N mutation in the RNA-binding domain in cultured hippocampal neurons. *Cellular and Molecular Neurobiology* **21**, 29-38.

Cheever, A. and Ceman, S. (2009). Phosphorylation of FMRP inhibits association with Dicer. *RNA*, **15**, 362-366.

Chen, S. L., Loffler, K. A., Chen, D., Stallcup, M. R. and Muscat, G. E. O. (2002). The coactivator-associated arginine methyltransferase Is necessary for muscle differentiation. CARM1 coactivates myocyte enhancer factor-2. *J. Biol. Chem.* **277**, 4324-4333.

Cougot, N., Babajko, S. and Seraphin, B. (2004). Cytoplasmic foci are sites of mRNA decay in human cells. *J. Cell Biol.* **165**, 31-40.

Cougot, N., Bhattacharyya, S. N., Tapia-Arancibia, L., Bordonne, R., Filipowicz, W., Bertrand, E. and Rage, F. (2008). Dendrites of mammalian neurons contain

specialized P-body-like structures that respond to neuronal activation. *J. Neurosci.* **28**, 13793-13804.

Cziko, A.-M. J., McCann, C. T., Howlett, I. C., Barbee, S. A., Duncan, R. P., Luedemann, R., Zarnescu, D., Zinsmaier, K. E., Parker, R. R. and Ramaswami, M. (2009). Genetic modifiers of dFMR1 encode RNA-granule components in *Drosophila*. *Genetics* **182**, 1051-1060.

Darnell, J. C., Mostovetsky, O. and Darnell, R. B. (2005). FMRP RNA targets: identification and validation. *Genes, Brain and Behavior* **4**, 341-349.

Davidovic, L., Huot, M.-C. and Khandjian, E. (2004). Lost once, the fragile X mental retardation protein is now back on brain polyribosomes. *RNA Biology* **1**, 125-127.

De Diego Otero, Y., Severijnen, L.-A., van Cappellen, G., Schrier, M., Oostra, B. and Willemsen, R. (2002). Transport of fragile X mental retardation protein via granules in neurites of PC12 Cells. *Mol. Cell. Biol.* **22**, 8332-8341.

Detrich III, H. W. (2008). Fluorescent proteins in zebrafish cell and developmental biology. In *Fluorescent Proteins*, vol. 85 (ed. K. F. Sullivan), pp. 220-237. San Diego: Academic Press.

Di Giorgi, F., Ahmed, Z., Bastianutto, C., Brini, M., Jouaville, S., Marsault, R., Murgia, M., Pinton, P., Pozzan, T. and Rizzuto, R. (1999). Targeting GFP to organelles. In *Green Fluroescent Proteins*, vol. 58 (eds K. F. Sullivan and S. A. Kay), pp. 75-85. San Diego: Academic Press.

Dictenberg, J. B., Swanger, S. A., Antar, L. N., Singer, R. H. and Bassell, G. J. (2008). A direct role for FMRP in activity-dependent dendritic mRNA transport links

filopodial-spine morphogenesis to fragile X syndrome. *Developmental Cell* **14**, 926-939.

Didiot, M.-C., Subramanian, M., Flatter, E., Mandel, J.-L. and Moine, H. (2008). Cells lacking the fragile X mental retardation protein (FMRP) have normal RISC activity but exhibit altered stress granule assembly. *Mol. Biol. Cell* **20**, 428-437.

Dolzhanskaya, N., Merz, G., Aletta, J. M. and Denman, R. B. (2006a). Methylation regulates FMRP's intracellular protein-protein and protein-RNA interactions. *J Cell Sci* **119**, 1933-1946.

Dolzhanskaya, N., Merz, G. and Denman, R. B. (2006b). Oxidative stress reveals heterogeneity of FMRP granules in PC12 cell neurites. *Brain Research* **1112**, 56-64.

Encinas, J. M. and Enikolpov, G. (2008). Identifying and quantifying neural stem cell and progenitor cells in the adult brain. In *Fluorescent Proteins*, vol. 85 (ed. K. F. Sullivan), pp. 244-270. San Diego: Academic Press.

Gay, D. A., Sisodia, S. S. and Cleveland, D. W. (1989). Autoregulatory control of beta-tubulin mRNA stability is linked to translation elongation. *Proceedings of the National Academy of Sciences of the United States of America* **86**, 5763-5767.

González-González, E., López-Casas, P. P. and del Mazo, J. (2008). The expression patterns of genes involved in the RNAi pathways are tissue-dependent and differ in the germ and somatic cells of mouse testis. *Biochimica et Biophysica Acta (BBA) - Gene Regulatory Mechanisms* **1779**, 306-311.

Grollman, A. P. and Huang, M. T. (1976). Protein Synthesis. New York: Marcel Dekker.

Hengst, U., Cox, L. J., Macosko, E. Z. and Jaffrey, S. R. (2006). Functional and selective RNA interference in developing axons and growth cones. *J. Neurosci.* **26**, 5727-5732.

Hou, L., Antion, M. D., Hu, D., Spencer, C. M., Paylor, R. and Klann, E. (2006). Dynamic translational and proteasomal regulation of fragile X mental retardation protein controls mGluR-dependent Long-Term Depression. *Neuron* **51**, 441-454.

Ishizuka, A., Siomi, M. C. and Siomi, H. (2002). A Drosophila fragile X protein interacts with components of RNAi and ribosomal proteins. *Genes Dev* **16**, 2497-508.

Kanai, Y., Dohmae, N. and Hirokawa, N. (2004). Kinesin transports RNA: isolation and characterization of an RNA-transporting granule. *Neuron* **43**, 513-525.

Kedersha, N., Anderson, P. and Jon, L. (2007). Mammalian stress granules and processing bodies. In *Methods in Enzymology*, vol. Volume 431, pp. 61-81: Academic Press.

Kedersha, N., Chen, S., Gilks, N., Li, W., Miller, I. J., Stahl, J. and Anderson, P. (2002). Evidence that ternary complex (eIF2-GTP-tRNAiMet)-deficient preinitiation complexes are core constituents of mammalian stress granules. *Mol. Biol. Cell* **13**, 195-210.

Kedersha, N., Cho, M. R., Li, W., Yacono, P. W., Chen, S., Gilks, N., Golan, D. E. and Anderson, P. (2000). Dynamic shuttling of TIA-1 accompanies the recruitment of mRNA to mammalian stress granules. *J. Cell Biol.* **151**, 1257-1268.

Kedersha, N., Stoecklin, G., Ayodele, M., Yacono, P., Lykke-Andersen, J., Fitzler, M. J., Scheuner, D., Kaufman, R. J., Golan, D. E. and Anderson, P. (2005). Stress

granules and processing bodies are dynamically linked sites of mRNP remodeling. *J. Cell Biol.* **169**, 871-884.

Kedersha, N., Tisdale, S., Hickman, T., Anderson, P., Maquat, L., E. and Kildjian, M. (2008). Real-time and quantitative imaging of mammalian stress granules and processing bodies. In *Methods in Enzymology*, vol. Volume 448, pp. 521-552: Academic Press.

Kimball, S. R., Horetsky, R. L., Ron, D., Jefferson, L. S. and Harding, H. P. (2003). Mammalian stress granules represent sites of accumulation of stalled translation initiation complexes. *Am J Physiol Cell Physiol* **284**, C273-284.

Kwon, S., Zhang, Y. and Matthias, P. (2007). The deacetylase HDAC6 is a novel critical component of stress granules involved in the stress response. *Genes & Development* **21**, 3381-3394.

Levenga, J., Buijsen, R. A. M., Rifé, M., Moine, H., Nelson, D. L., Oostra, B. A., Willemsen, R. and de Vrij, F. M. S. (2009). Ultrastructural analysis of the functional domains in FMRP using primary hippocampal mouse neurons. *Neurobiology of Disease* **35**, 241-250.

Lindqvist, L., Oberer, M., Reibarkh, M., Cencic, R., Bordeleau, M.-E., Vogt, E., Marintchev, A., Tanaka, J., Fagotto, F., Altmann, M. et al. (2008). Selective pharmacological targeting of a DEAD box RNA helicase. *PLoS ONE* **3**, e1583.

Ling, S.-C., Fahrner, P. S., Greenough, W. T. and Gelfand, V. I. (2004). Transport of Drosophila fragile X mental retardation protein-containing ribonucleoprotein granules by kinesin-1 and cytoplasmic dynein. *Proc Nat'l Acad Sci* **101**, 17428-17433.

Lippincott-Schwartz, J., Presley, F., Zaal, K. J. M., Hirschberg, K., Miller, C. D. and Ellenberg, J. (1999). Monitoring the dynamics of membrane proteins tagged with green fluorescent protein. In *Green Fluroescent Proteins*, vol. 58 (eds K. F. Sullivan and S. A. Kay), pp. 261-280. San Diego: Academic Press.

Lu, L., Han, A.-P. and Chen, J.-J. (2001). Translation initiation control by heme-regulated eukaryotic initiation factor 2alpha kinase in erythroid cells under cytoplasmic stresses. *Mol. Cell. Biol.* **21**, 7971-7980.

Mazroui, R., Di Marco, S., Kaufman, R. J. and Gallouzi, I.-E. (2007). Inhibition of the ubiquitin-proteasome system induces stress granule formation. *Mol. Biol. Cell* **18**, 2603-2618.

Mazroui, R., Huot, M.-E., Tremblay, S., Filion, C., Labelle, Y. and Khandjian, E. W. (2002). Trapping of messenger RNA by fragile X mental retardation protein into cytoplasmic granules induces translation repression. *Hum. Mol. Genet.* **11**, 3007-3017.

Mazroui, R., Sukarieh, R., Bordeleau, M.-E., Kaufman, R. J., Northcote, P., Tanaka, J., Gallouzi, I. and Pelletier, J. (2006). Inhibition of ribosome recruitment induces stress granule formation independent of eIF2{alpha} phosphorylation. *Mol. Biol. Cell* **17**, 4212-4219.

McEwen, E., Kedersha, N., Song, B., Scheuner, D., Gilks, N., Han, A., Chen, J.-J., Anderson, P. and Kaufman, R. J. (2005). Heme-regulated inhibitor kinase-mediated phosphorylation of eukaryotic translation initiation factor 2 inhibits translation, induces stress granule formation, and mediates survival upon arsenite exposure. *J. Biol. Chem.* **280**, 16925-16933.

Minagawa, K., Katayama, Y., Nishikawa, S., Yamamoto, K., Sada, A., Okamura, A., Shimoyama, M. and Matsui, T. (2009). Inhibition of G1 to S phase progression by a novel zinc finger protein p58TFL at P-bodies. *Molecular Cancer Research* **7**, 880-889.

Minagawa, K. and Matsui, T. (2010). p58TFL does not localize to messenger RNA processing bodies - Response. *Molecular Cancer Research* **8**, 132-133.

Özlü, N., Srayko, M., Kinoshita, K., Habermann, B., O Toole, E. T., Müller-Reichert, T., Schmalz, N., Desai, A. and Hyman, A. A. (2005). An essential function of the C. elegans ortholog of TPX2 is to localize activated Aurora A kinase to mitotic spindles. *Dev. Cell* **9**, 237-248.

Pfeiffer, B. E. and Huber, K. M. (2007). Fragile X mental retardation protein induces synapse loss through acute postsynaptic translational regulation. *J. Neurosci.* **27**, 3120-3130.

Piazzon, N., Rage, F., Schlotter, F., Moine, H., Branlant, C. and Massenet, S. (2007). In vitro and in cellulo evidences for association of the survival of motor neuron complex with the fragile X mental retardation protein. *J. Biol. Chem.* **283**, 5598-5610.

Pierce, D. and Vale, R. D. (1999). Single-molecule fluorescence detection of green fluorescent protein and application to single protein dynamics. In *Green Fluroescent Proteins*, vol. 58 (eds K. F. Sullivan and S. A. Kay), pp. 49-72. San Diego: Academic Press.

Querido, E. and Chartrand, P. (2008). Using fluorescent proteins to study mRNA trafficking in living cells. In *Fluorescent Proteins*, vol. 85 (ed. K. F. Sullivan), pp. 274-291. San Diego: Academic Press.

Rackham, O. and Brown, C. E. (2004). Visualization of RNA-protein interactions in living cells: FMRP and IMP1 interact on mRNAs. *EMBO J* **23**, 3346-3355.

Solomon, S., Xu, Y., Wang, B., David, M. D., Schubert, P., Kennedy, D. and Schrader, J. W. (2007). Distinct structural features of caprin-1 mediate its interaction with G3BP-1 and its induction of phosphorylation of eukaryotic translation initiation factor 2{alpha}, entry to cytoplasmic stress granules, and selective interaction with a subset of mRNAs. *Mol. Cell. Biol.* **27**, 2324-2342.

Swiercz, R., Cheng, D., Kim, D. and Bedford, M. T. (2007). Ribosomal protein rpS2 is hypomethylated in PRMT3-deficient mice. *J. Biol. Chem.* **282**, 16917-16923.

Swiercz, R., Person, M. D. and Bedford, M. T. (2004). Ribosomal protein S2 is a substrate for mammalian protein arginine methyltransferase 3 (PRMT3). *Biochemical Journal* **386**, 85-91.

Thomas, M. G., Martinez Tosar, L. J., Loschi, M., Pasquini, J. M., Correale, J., Kindler, S. and Boccaccio, G. L. (2004). Staufen recruitment into stress granules does not affect early mRNA transport in oligodendrocytes. *Mol. Biol. Cell* **16**, 405-420.

Wang, H., Dictenberg, J. B., Ku, L., Li, W., Bassell, G. J. and Feng, Y. (2008). Dynamic association of the fragile X mental retardation protein as a messenger ribonucleoprotein between microtubules and polyribosomes. *Mol. Biol. Cell* **19**, 105-114.

Wasserman, T., Katsenelson, K., Daniliuc, S., Hasin, T., Choder, M. and Aronheim, A. (2009). A novel JNK binding protein WDR62 is recruited to stress granules and mediates a non-classical JNK activation. *Mol. Biol. Cell* **21**, 117-130.

White, J. P., Cardenas, A. M., Marissen, W. E. and Lloyd, R. E. (2007). Inhibition of cytoplasmic mRNA stress granule formation by a viral proteinase. *Cell Host & Microbe* **2**, 295-305.

Xie, W., Dolzhanskaya, N., LaFauci, G., Dobkin, C. and Denman, R. B. (2009). Tissue and developmental regulation of fragile X mental retardation protein exon 15 isoforms. *Neurobiology of Disease* **35**, 52-62.

Yamasaki, S., Stoecklin, G., Kedersha, N., Simarro, M. and Anderson, P. (2007). T-cell intracellular antigen-1 (TIA-1)-induced translational silencing promotes the decay of selected mRNAs. *Journal of Biological Chemistry* **282**, 30070-30077.

Zhang, H., Xing, L., Rossoll, W., Wichterle, H., Singer, R. H. and Bassell, G. J. (2006). Multiprotein complexes of the survival of motor neuron protein SMN with gemins traffic to neuronal processes and growth cones of motor neurons. *J. Neurosci.* **26**, 8622-8632.

Legends

Fig. 1. EGFP-FMRP granules are heterogeneous. (A) Confocal images of HeLa cells expressing EGFP-FMRP, EGFP, or endogenous FMRP. **(B)** Size distribution of EGFP-FMRP granules in HeLa cells. Analysis was based on 9 transfected cells. Note the three classes of granules (small, intermediate, large) based on size. **(C)** Size distribution of endogenous FMRP granules. Analysis was based on 27 cells. Comparison of the two distributions shows that endogenous FMRP granules are significantly smaller ($P<0.00084$).

Fig. 2. EGFP-FMRP granules partially colocalize with the stress granule marker TIA1. Panels a-c show EGFP-FMRP (green), TIA1 (red) and merged images of

transfected PC12 cells. Panels d-i show comparable images of transfected HeLa cells expressing EGFP-FMRP.

Fig. 3. EGFP-FMRP granules partially colocalize with the stress granule marker FXR1P. **(A)** Panels a-c show endogenous FRMP (green), endogenous FXR1P (red) and merged images of HeLa cells treated with 0.5 mM arsenite for 20 minutes. Boxed areas show magnified views of select FMRP granules reveal the near complete colocalization of the granules. **(B)** Panels d-f show EGFP-FMRP (green), endogenous FXR1P (red) and merged images of transfected HeLa cells. Boxed areas show magnified views of select EGFP-FMRP granules. White arrows mark FXR1P-only granules; yellow arrows mark colocalized granules and green arrows mark EGFP-FMRP-only granules. **(C)** Panels g-i show EGFP-FMRP (green), endogenous FXR1P (red) and merged images of transfected HeLa cells treated with 0.5 mM arsenite for 20 minutes, 24 hours post-transfection. Boxed areas show magnified views of select EGFP-FMRP granules. White arrows mark FXR1P-only granules; yellow arrows mark colocalized granules and green arrows mark EGFP-FMRP-only granules.

Fig. 4. EGFP-FMRP granule formation does not require eIF2α phosphorylation. **(A)** Panels a-c show EGFP-FMRP (green), phospho-eIF2α (red) and merged images of transfected HeLa cells. Boxed areas show magnified views of select EGFP-FMRP granules. **(B)** Panels d-f show TIA1 (red), phospho-eIF2α (green) and merged images of HeLa cells treated with 0.5 mM arsenite for 20 minutes, 24 hours post-transfection. Boxed areas show magnified views of select TIA1 granules. Yellow arrows mark colocalized granules and red arrows mark TIA1 stress granules.

Fig. 5. Hippurstanol treatment recruits EGFP-FMRP into stress granules. (A) Panels a-c show EGFP-FMRP (green), TIA1 (red) and merged images of transfected HeLa cells treated with 10 μM hippurstanol for 30 minutes, 24 hours post-transfection. Boxed areas show magnified views of select EGFP-FMRP granules. Yellow arrows show colocalizing granules. Panels d-f show comparable images of EGFP-FMRP (green), phospho-eIF2α (red) and merged images of transfected HeLa cells treated with 10 μM hippurstanol for 30 minutes, 24 hours post-transfection. Boxed areas show magnified views of select EGFP-FMRP granules. Green arrows show non-colocalized granules. **(B)** Panels g-i show EGFP-FMRP (green), TIA1 (red) and merged images of transfected untreated HeLa cells. Boxed areas show magnified views of select EGFP-FMRP granules. Yellow arrows show colocalizing granules. Panels j-l show comparable images of EGFP-FMRP (green), phospho-eIF2α (red) and merged images of transfected untreated HeLa cells. Boxed areas show magnified views of select EGFP-FMRP granules. Yellow arrows show colocalizing granules green arrows show non-colocalized granules.

Fig. 6. EGFP-FMRP granules partially colocalize with the P-body marker protein Dcp1a. **(A)** Panels a-c show EGFP-FMRP (green), Dcp1a (red) and merged images of transfected untreated HeLa cells. Boxed areas presented below show magnified views of select EGFP-FMRP granules. Red arrows mark Dcp1a-only granules; yellow arrows mark colocalized granules and green arrows mark EGFP-FMRP-only granules. **(B)** Panels d-f show comparable images of transfected HeLa cells treated with 0.5 mM arsenite for 20 minutes, 24 hours post-transfection. Boxed areas presented below show magnified views of select EGFP-FMRP granules. Red arrows mark Dcp1a-only

granules; yellow arrows mark colocalized granules and green arrows mark EGFP-FMRP-only granules. **(C)** Panels g-i show TIA1 (green), Hsp70 (red) and merged images of transfected untreated HeLa cells. Panels j-l show comparable images of transfected HeLa cells treated with 0.5 mM arsenite for 20 minutes, 24 hours post-transfection. Boxed areas presented below show magnified views of select stress granules. Red arrows mark Hsp70-only granules; yellow arrows mark colocalized granules and green arrows mark TIA1-only granules.

Fig. 7. Endogenous TIA1 and endogenous FMRP stress granules respond to emetine. (A) Panels a-d show endogenous TIA1 (red), endogenous FMRP (green) HeLa cells treated with 0.5 mM arsenite for 20 minutes or treated with 0.5 mM arsenite and then 10 μg/ml of emetine for 1 hour. Boxed areas presented below show magnified views of select stress granules. Size distribution of HeLa cell endogenous **(B)** TIA1 **(C)** endogenous FMRP stress granules in the presence and absence of emetine. Analysis was based on 10 cells for each protein. Comparison of the two distributions shows that emetine significantly reduces the size of both classes of stress granules ($P<0.049$ and $P< 4.5x10^{-6}$, respectively).

Fig. 8. EGFP-FMRP granules respond to emetine. (A) Panels a-d show EGFP-FMRP granules (green) in untreated HeLa cells (a, b) or HeLa cells treated with 0.5 mM arsenite for 20 minutes or treated with 0.5 mM arsenite and then 10 μg/ml of emetine for 1 hour (c, d). All treatments were performed 24 hours post-transfection. Boxed areas presented below show magnified views of select stress granules. Size distribution of HeLa cell EGFP-FMRP granules in the absence or presence of emetine and in the **(B)** absence or **(C)** presence of arsenite. Analysis was based on 10 transfected cells for each protein.

Comparison of the two distributions shows that emetine significantly reduces the size of both classes of stress granules ($P< 0.00084$ and $P< 0.0023$, respectively).

Fig. 9. EGFP-FMRP granules are dynamic. (A) Pseudo colored image of EGFP-FMRP expressing HeLa cell. White box shows a region of interest (ROI) prior to photobleaching, while the yellow boxes show comparable ROIs of unbleached EGFP-FMRP granules. Arrows point to a granule that was photobleached (PB) and a nearby control granule (Ctrl) that was not. **(B)** Time-dependent changes in the intensity of the ROIs shown in **(A)**. **(C)** Time-dependent changes in PB (upper) and Ctrl (lower) granules shown in **(A)**. **(D)** Effect of arsenite treatment on EGFP-FMRP photobleaching recovery rates. The intensity at time 0 for 25 non-bleached EGFP-FMRP granules, 23 arsenite-treated photobleached EGFP-FMRP granules and 39 photobleached untreated EGFP-FMRP granules from 5 different cells was plotted. The difference between the photobleached arsenite-treated granules was not significantly different from the untreated granules ($P>0.2$, ANOVA). For presentation clarity error bars are shown on every third time point.

Fig. 10. EGFP-FMRP granules contain asymmetrically dimethylated proteins. **(A)** HeLa cells expressing EGFP-FMRP were immunostained with antibodies directed to asymmetrically dimethylated proteins. Panels a-e show images of EGFP-FMRP (green), ASYM24 (red), and their merged counterpart whereas panels f-k show images of EGFP-FMRP (green), mRG (red), and their merged counterpart. Panels l-m demonstrate lack of immunostaining in the absence of primary antibody. As indicated, the cells were either treated or not treated with 20 μM AdOx for 24 hour following transfection. **(B)** Quantification of anti-ASYM24 pAb, anti-mRG pAb and anti-SYM10 immunostaining in

HeLa cells grown in the absence (-) or presence (+) of 20 μM AdOx. The fluorescence intensity of the individual cells was determined using the histogram function in Adobe Photoshop as previously described (Dolzhanskaya et al., 2006a). The values for 50-75 cells/antibody for each treatment are plotted. The reduction in fluorescence intensity in the presence of AdOx was significantly less than in its absence (ASYM24 $P< 5x10^{-15}$, mRG $P< 4x10^{-15}$, SYM10 $P< 5x10^{-17}$ ANOVA).

Fig. 11. EGFP-FMRP granule expression does not require full protein methylation. **(A)** HeLa cells were either treated or not treated with 20 μM AdOx for 24 hours prior to transfection. Subsequently, the cells were transfected with pEGFP-FMRP and imaged 24 hours later. Note: AdOx was re-applied to the set of cells that were pre-treated with AdOx. **(B)** Size distribution of HeLa cell arsenite-treated EGFP-FMRP granules in the presence and absence of AdOx. Analysis was based on 10 transfected cells/treatment. Comparison of the two distributions shows that AdOx does not significantly reduce the size of EGFP-FMRP granules ($P> 0.4$).

Fig. 12. EGFP-FMRP granules contain symmetrically dimethylated proteins. **(A)** HeLa cells expressing EGFP-FMRP were immunostained with an antibody directed to symmetrically dimethylated proteins (sDMA), SYM10. Panels a-f show images of EGFP-FMRP (green), sDMA (red), and their merged counterparts in untreated cells and cells treated with 20 μM AdOx for 24 hours following transfection. Panels g-l show cells comparably treated cells that were either treated or not treated with 0.5 mM arsenite for 20 minutes, 24 hours post-transfection. **(B)** Boxed areas from **(A)** show magnified views of select cells; yellow arrows mark colocalizing granules, green arrows mark EGFP-FMRP only granules and red arrows mark sDMA only granules.

Fig. 13. AdOx inhibits cellular methylation of proteins that colocalize in EGFP-FMRP granules. Representative Western blots of HeLa cell proteins (30 μg) probed with antibodies directed to methylated proteins, ASYM24 pAb (left) and SYM10 pAb (right), protein arginine methyltransferases (PRMTs) 1, 3, 4, and 5 and various load controls.

Fig. 14. Endogenous TIA1 stress granules contain sDMA proteins. HeLa cells were treated with 0.5 mM sodium arsenite (panels a-c) or not treated panels (e-g). Subsequently, the cells were immunostained with antibodies that detect the stress granule marker TIA1 (red) and SYM10 (green) and subject to confocal microscopy. Magnified views of select regions of the upper panels are presented below to clearly show the granules. Large TIA1-containing stress granules that colocalize with symmetrically dimethylated proteins are marked with yellow arrows. These are contrasted with smaller granules harboring symmetrically dimethylated proteins, but which do not colocalize with TIA1 (green arrows). *Note that these smaller granules are constitutively present in untreated cells. We speculate that these may be related to the 7S PRMT5 complex, the 20S methylosome or the SMN complex.*

Fig. 15. Stress granules, EGFP-FMRP granules and endogenous FMRP granules do not contain SmD3. HeLa cells **(A**, **B)** and HeLa cells expressing EGFP-FMRP **(C)** were treated or not treated with 0.5 mM sodium arsenite, 24 hours post-transfection. Subsequently, the cells were immunostained with antibodies to FMRP (panels a, d), TIA1 (panels g, j) and SmD3 (panels b, e, h, k, n, q) and subject to confocal microscopy. Magnified views of select regions of the upper panels are presented below to clearly show the granules. In none of cases do SmD3 granules and the other markers truly

colocalize; however, in the arsenite treatments smaller SmD3 granules appear to be associated with some of the larger stress granules (yellow arrows).

Fig. 16. Stress granules, EGFP-FMRP granules and endogenous FMRP granules do not contain SmB/B'. HeLa cells **(A, B)** and HeLa cells expressing EGFP-FMRP **(C)** were treated or not treated with 0.5 mM sodium arsenite for 20 minutes. Subsequently, the cells were immunostained with antibodies to FMRP (panels a, d), TIA1 (panels g, j) and SmB/B' (panels b, e, h, k, n, q) and subject to confocal microscopy. Magnified views of select regions of the upper panels are presented below to clearly show the granules. In none of cases do SmB/B' granules and the other markers colocalize.

Fig. 17. PRMT3 colocalizes with FXR1P-containing stress granules. HeLa cells were treated for 20 minutes with 0.5 mM sodium arsenite, other cells were treated 24 hours with 10 μM AdOx, followed by 20 minutes with 0.5 mM sodium arsenite or left untreated. Subsequently, the cells were immunostained with an antibody that detects the stress granule marker FXR1P (red) and one that detects PRMT3 (green) and subject to confocal microscopy. FXR1P stress granules that colocalize with PRMT3 are indicated with yellow arrows.

Table 1. EGFP-FMRP Colocalization Analysis

Pair	Treatment	tM1[d]	tM2[d]
EGFP-FMRP/TIA1	None	0.069 (0.015)	0.057 (0.021)
	AdOx[a]	0.068 (0.023)	0.061 (0.007)
	Arsenite[b]	0.521 (0.014) †	0.449 (0.027) †
	Hippurstanol[c]	0.228 (0.028) †	0.373 (0.003) †
EGFP-FMRP/Dcp1a	None	0.024 (0.014)	0.007 (0.003)
	AdOx[a]	0.029 (0.011)	0.006 (0.003)
	Arsenite[b]	0.028 (0.003)	0.010 (0.005)
	Hippurstanol[c]	0.111 (0.045) †	0.126 (0.047) †

a. Treatment with 10 μM AdOx for 24 hrs prior to analysis.
b. Treatment with 0.5 mM sodium arsenite for 20 min. prior to analysis.
c. Treatment with 10 μM hippurstanol for 30 min. prior to analysis.
d. Thresholded Manders coefficients (Bolte and Cordelieres, 2006) for EGFP-FMRP granules, tM1 and tM2 were calculated using the JaCoP module in Image J. The means and standard deviations, shown in parentheses, for at least 25 transfected cells per treatment are presented; fluorescence from non-transfected cells in the field was manually masked in order to examine only the colocalization of EGFP-FMRP transfected cells.

†Treatment is significantly different from non-treated ($P>0.005$, ANOVA).

Table 2. Physical Characteristics of EGFP-FMRP Granules

Measure/Granule	EGFP-FMRP	Stress Granules[c]	Stress Granules[d]	P-bodies[e]
Circularity[a]	0.87 (0.2)†	0.91 (0.15)	0.91 (0.14)	0.95 (0.13)
Area[b]	16.2 (47) ‡	13.8 (29)	14.4 (19)	4.4 (8)

a. Circularity measures the deviation of the granule from a perfect circle, scored as 1; the mean and (standard deviation) are shown.
b. Area is given in squared pixels; the mean and (standard deviation) are shown.
c. HeLa cell arsenite-induced TIA1 granules.
d. HeLa cell hippurstanol-induced TIA1 granules.
d. HeLa cell endogenous Dcp1a granules.
† Circularity of 1000 EGFP-FMRP granules was significantly different from that of 1000 arsenite-induced granules, hippurstanol-induced granules and 1200 endogenous P-bodies ($P<1x10^{-32}$, ANOVA).
‡Area of 1000 EGFP-FMRP granules was significantly different from that of 1000 arsenite-induced granules, 1000 hippurstanol-induced granules and 1200 endogenous P-bodies ($P<6x10^{-19}$, ANOVA).

Nature Precedings : doi:10.1038/npre.2010.5442.1 : Posted 27 Dec 2010

Figure 1.

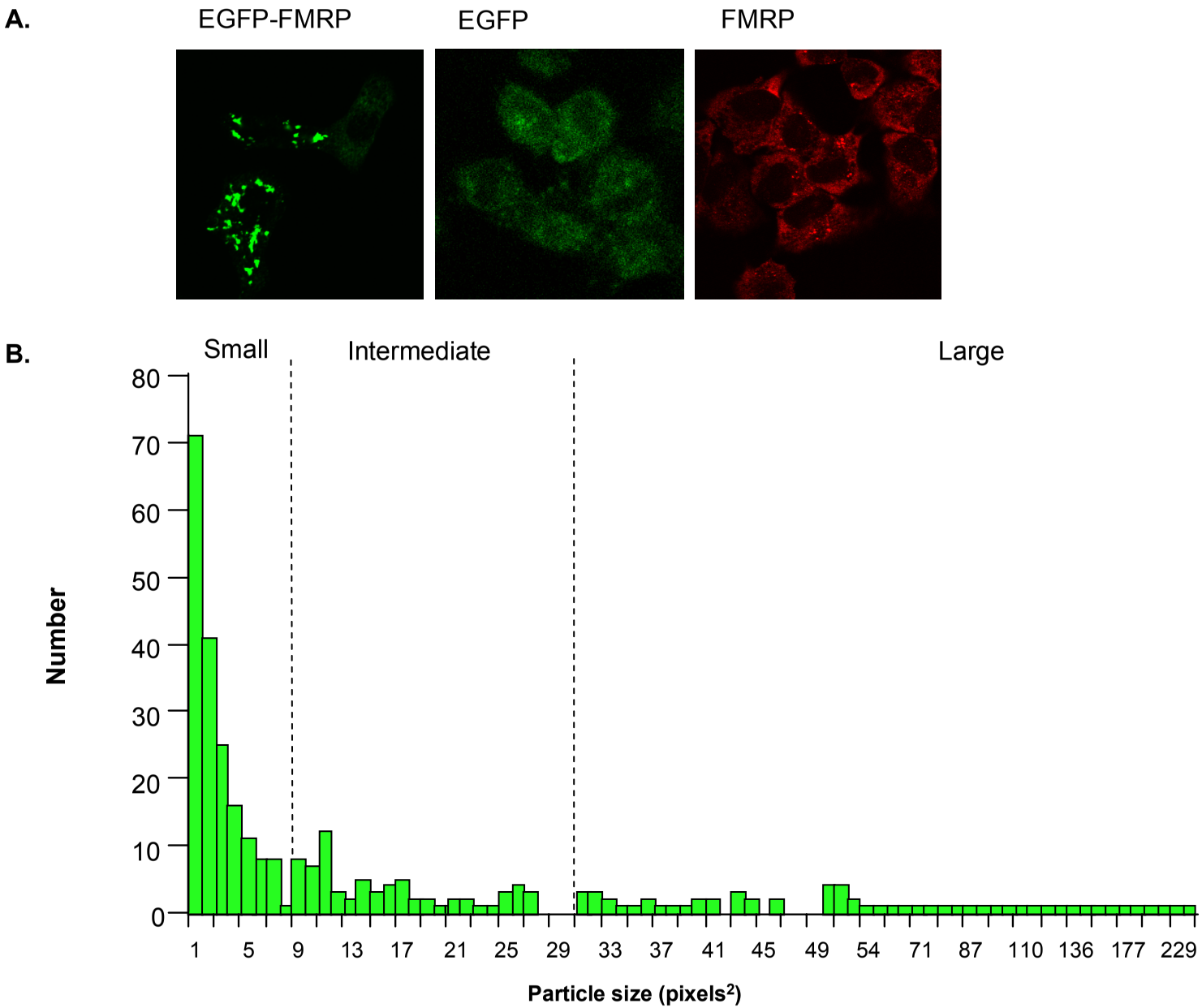

Nature Precedings : doi:10.1038/npre.2010.5442.1 : Posted 27 Dec 2010

Figure 1.

C.

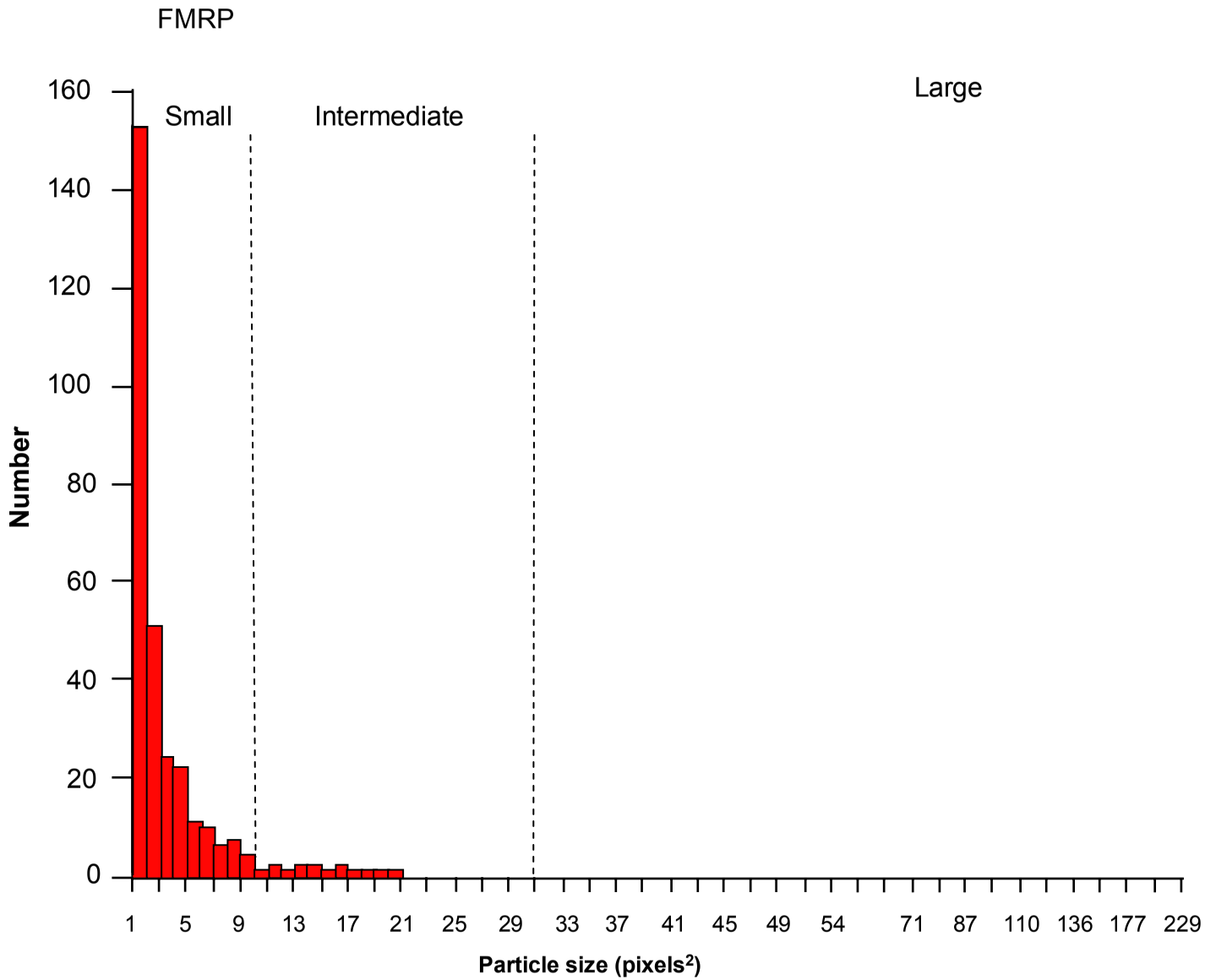

Figure 2

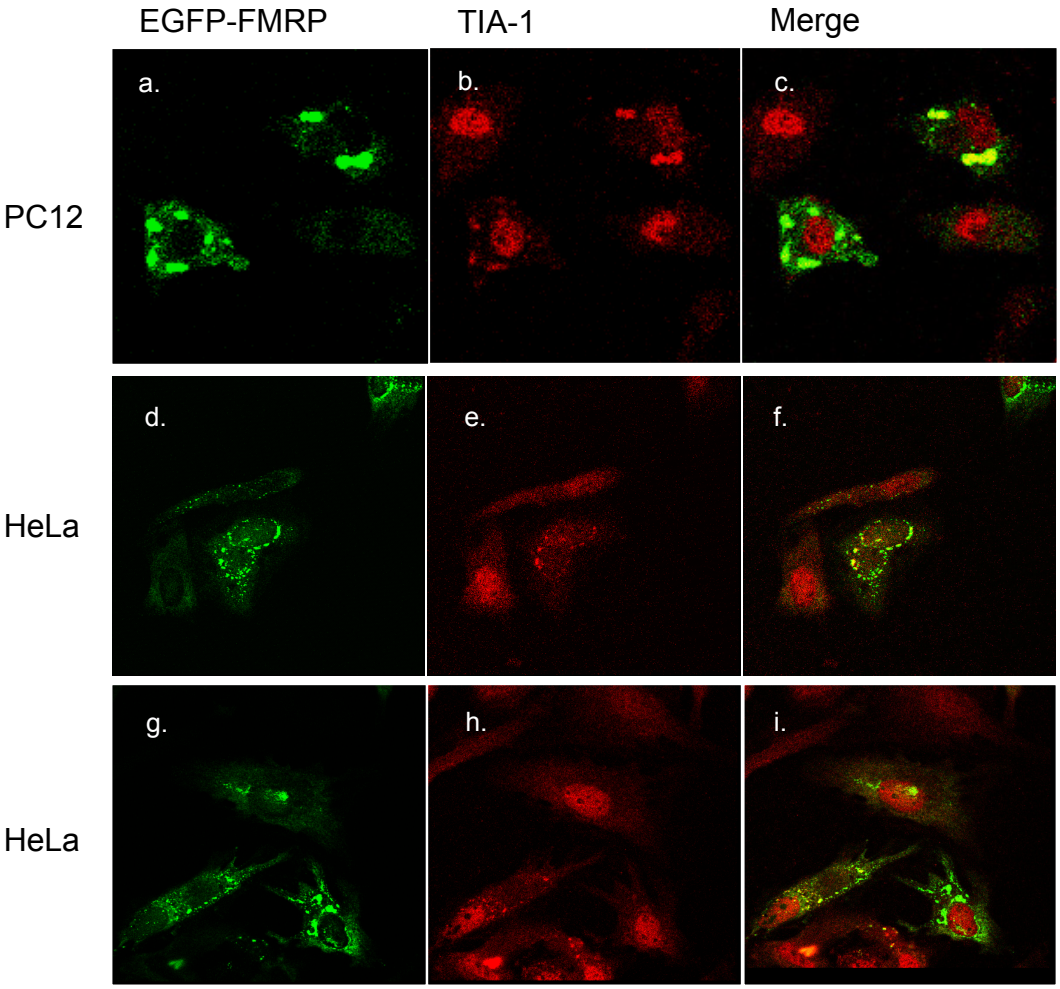

Figure 3.

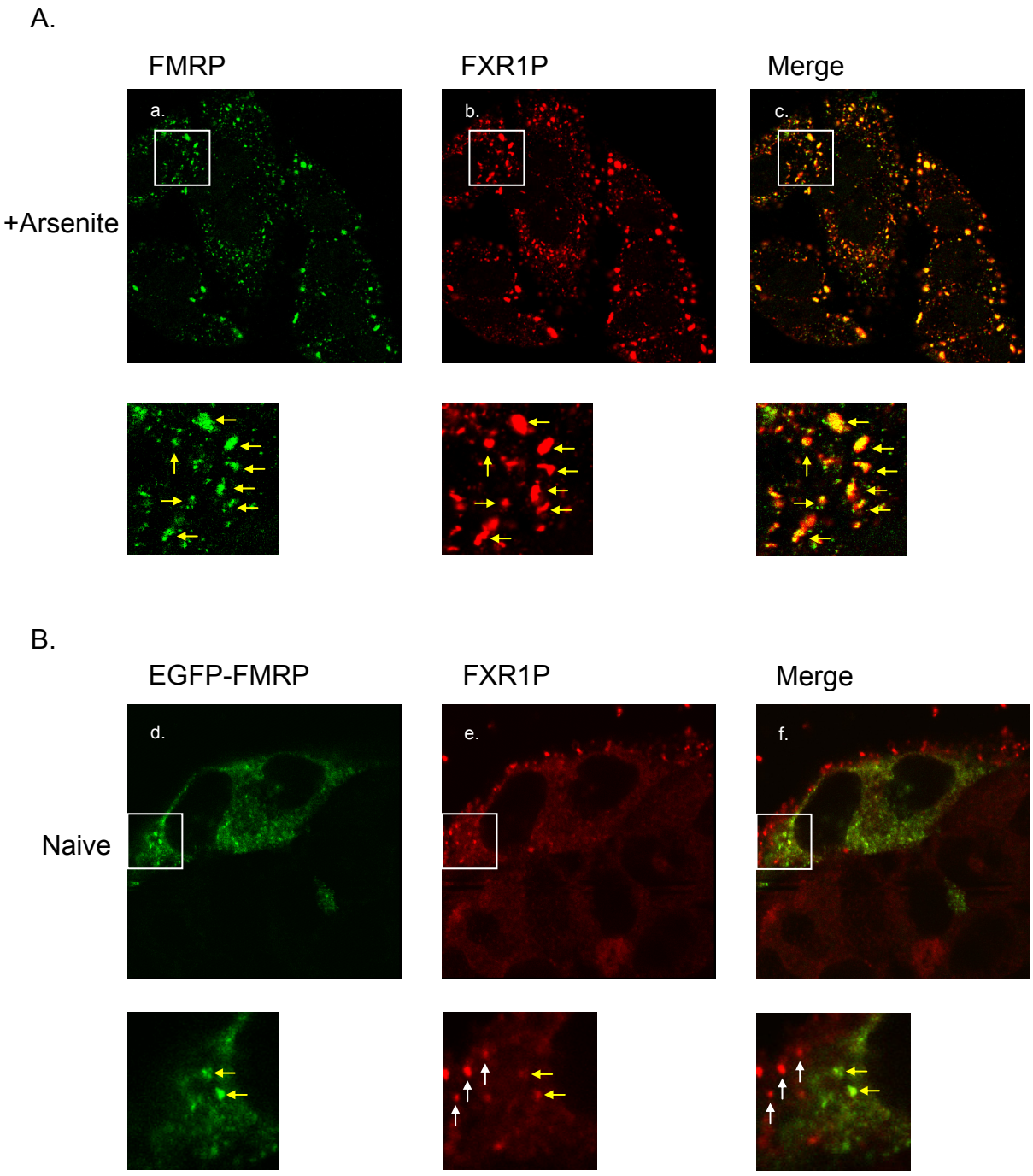

Figure 3.

C.

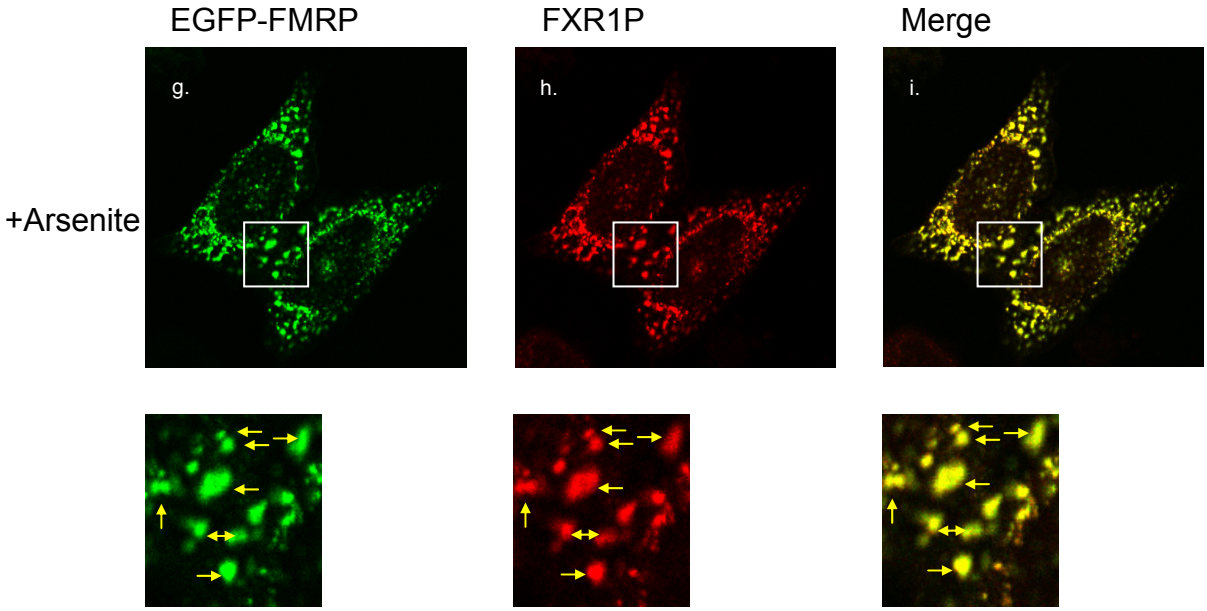

Figure 4.

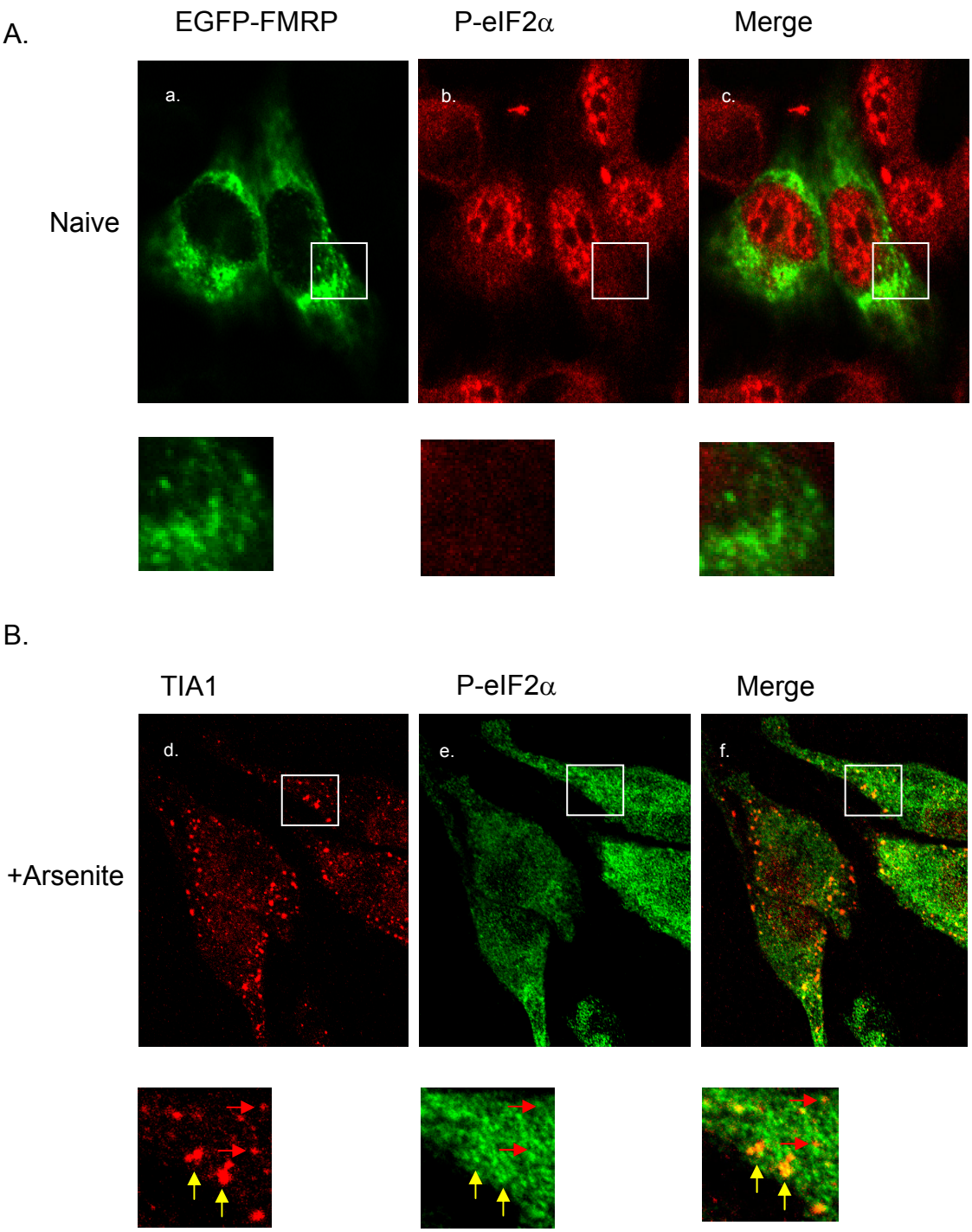

Figure 5.

A.

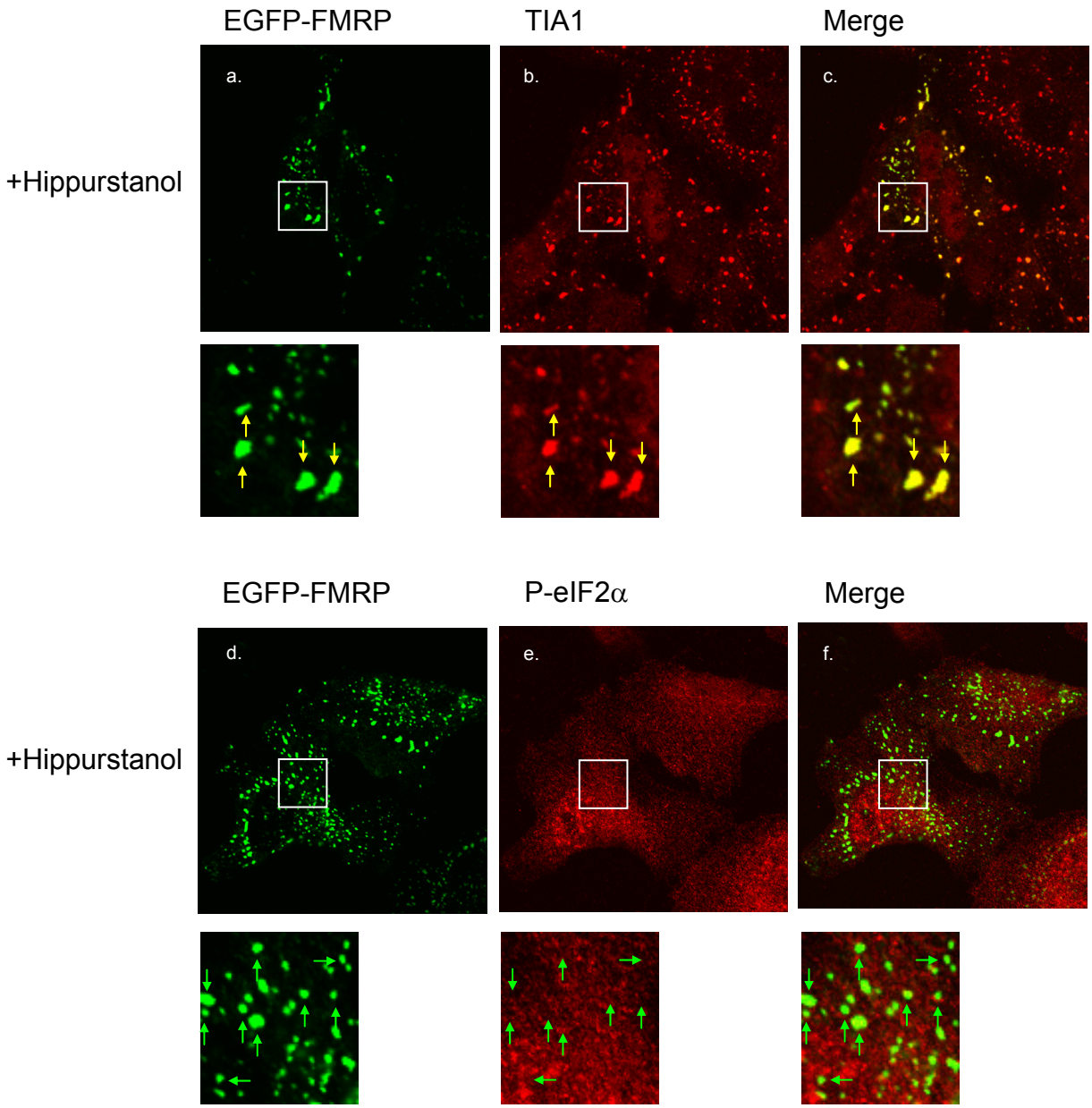

Figure 5.

B.

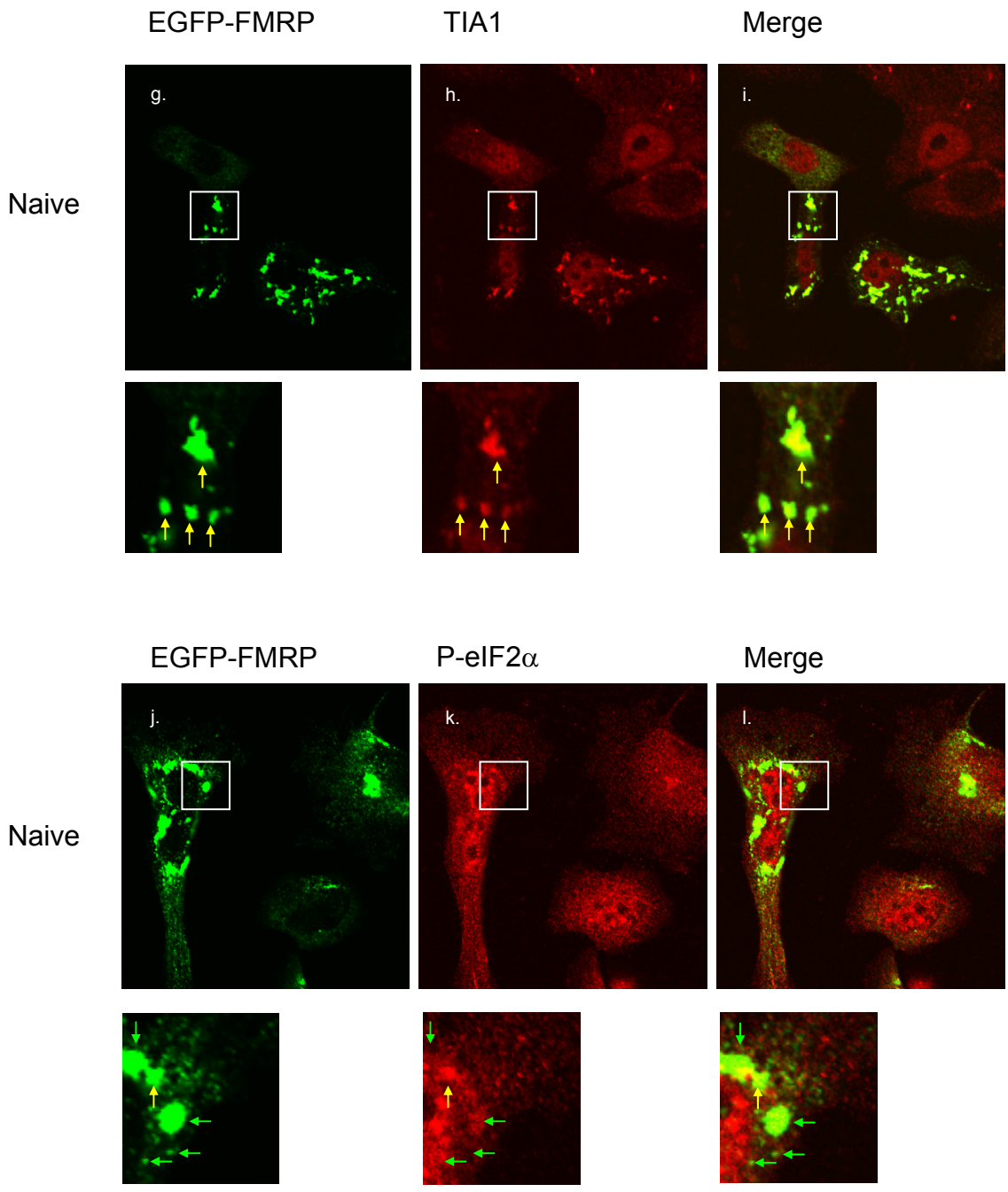

Figure 6.

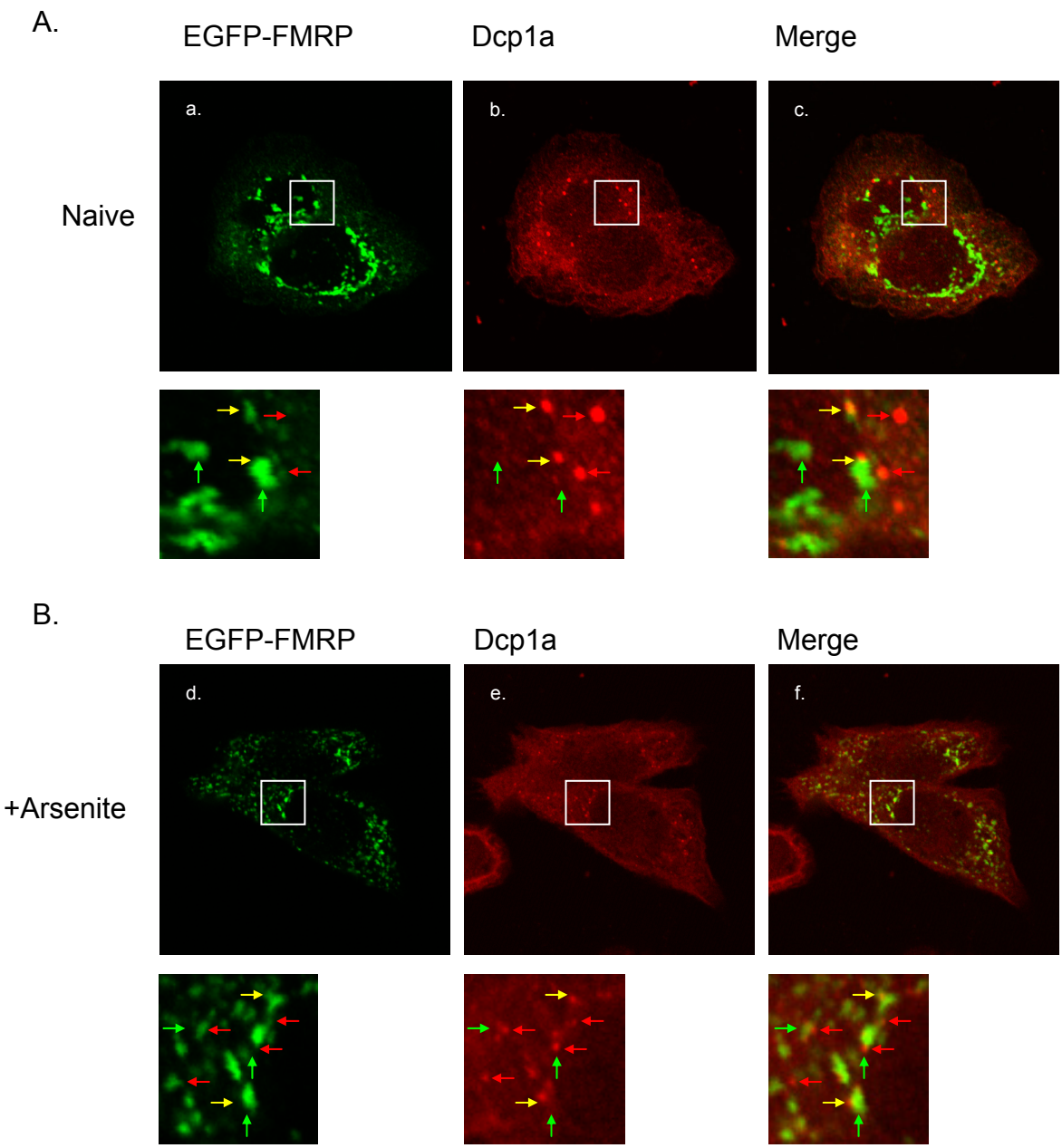

Figure 6.

C.

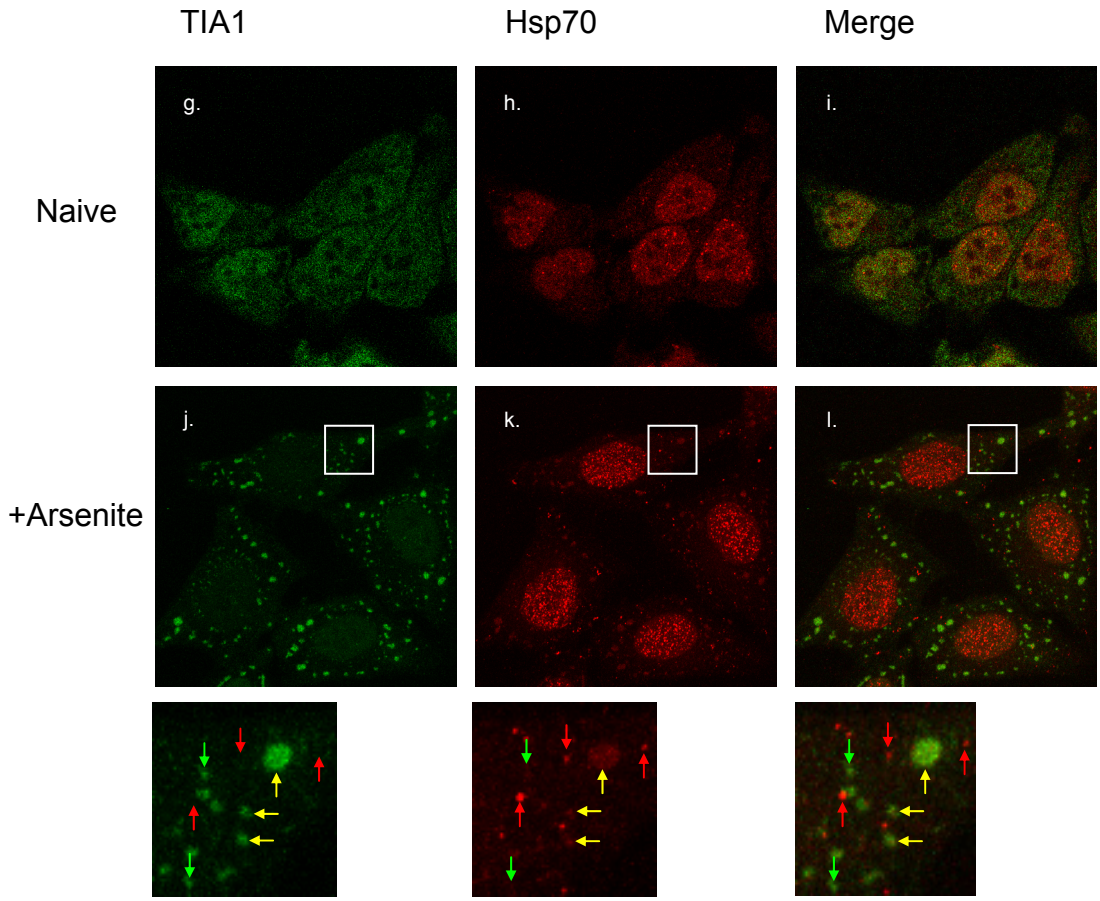

Nature Precedings : doi:10.1038/npre.2010.5442.1 : Posted 27 Dec 2010

Figure 7.

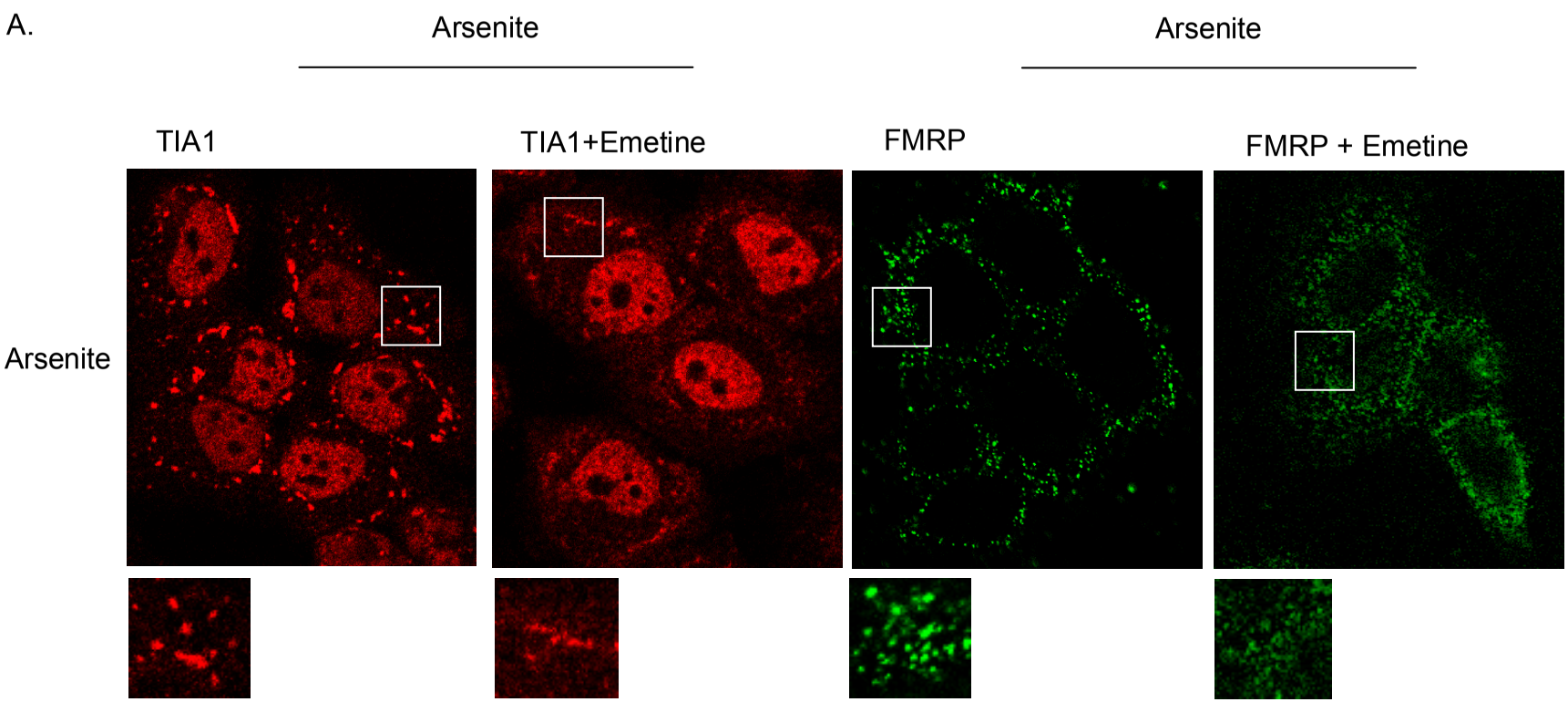

Nature Precedings : doi:10.1038/npre.2010.5442.1 : Posted 27 Dec 2010

Figure 7.

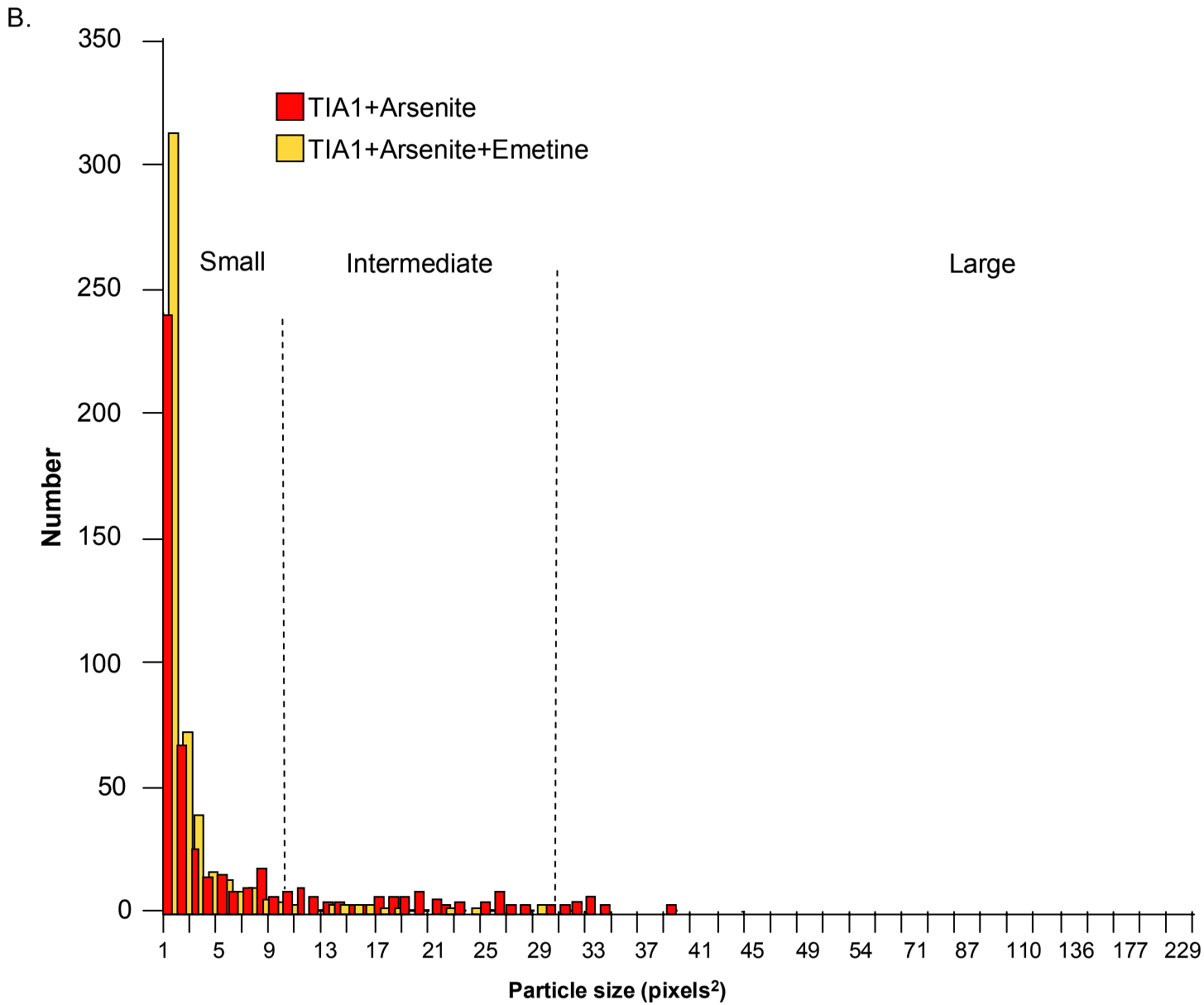

Nature Precedings : doi:10.1038/npre.2010.5442.1 : Posted 27 Dec 2010

Figure 7.

C.

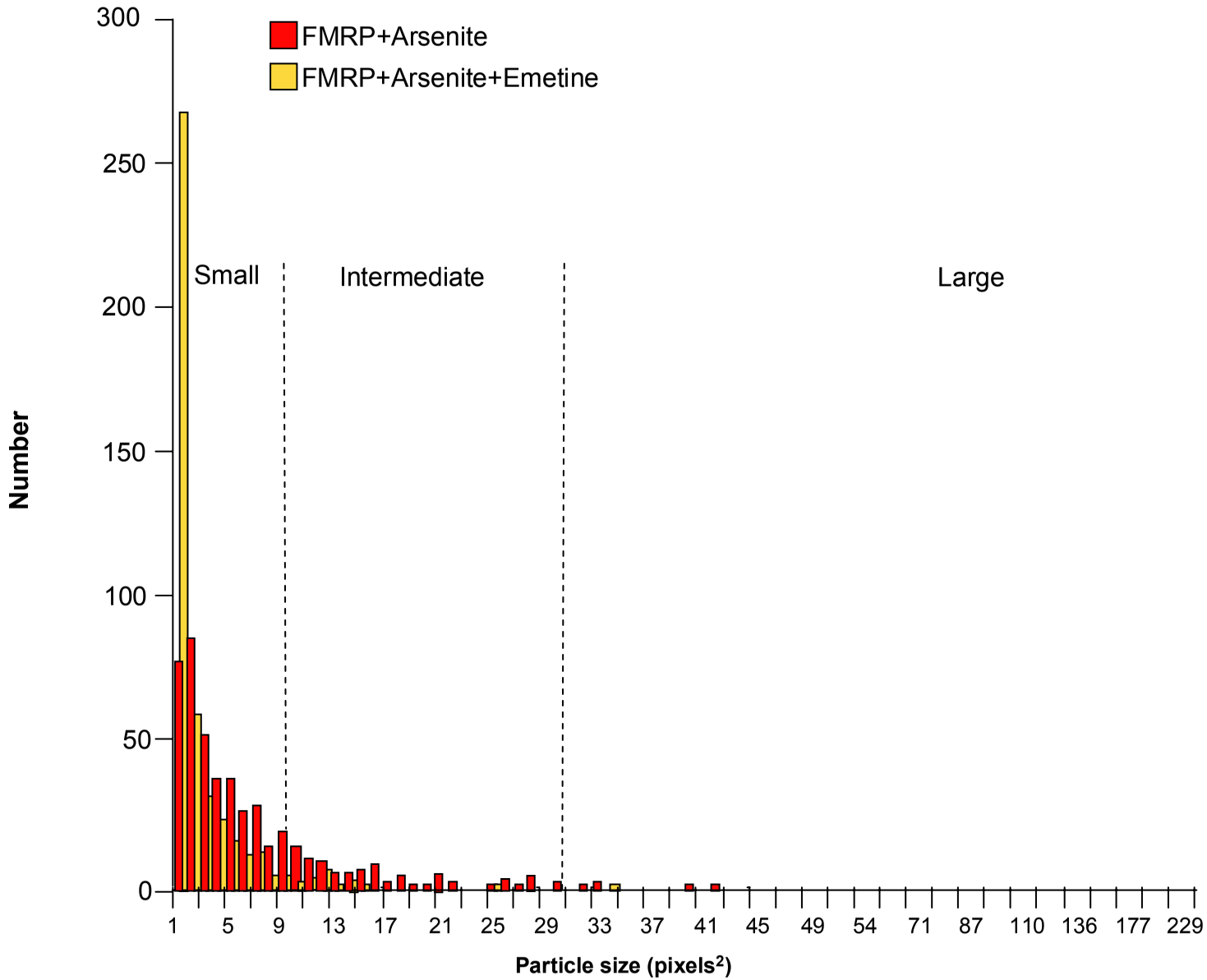

Figure 8.

A.

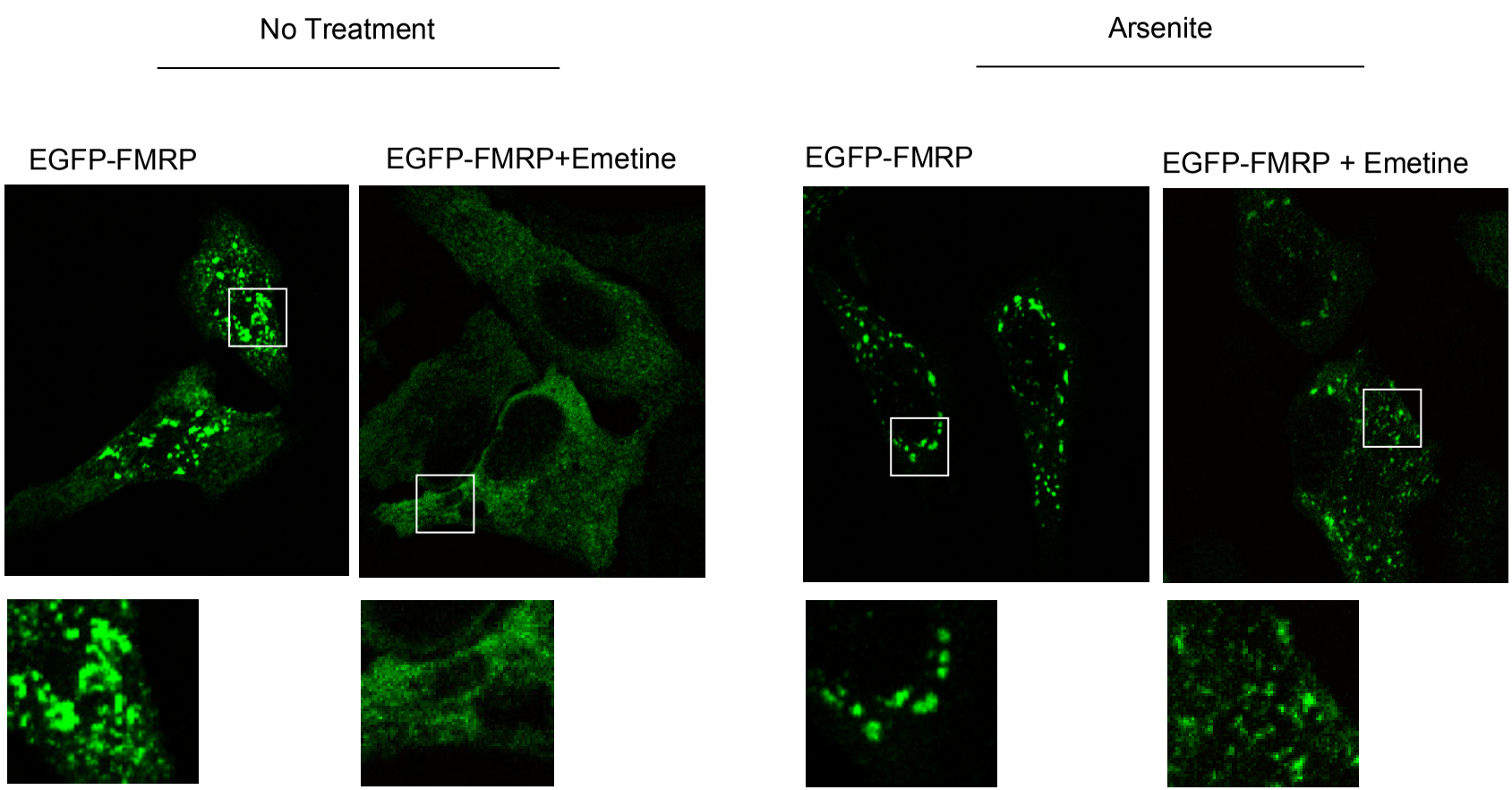
No Treatment
Arsenite
EGFP-FMRP
EGFP-FMRP+Emetine
EGFP-FMRP
EGFP-FMRP + Emetine

Nature Precedings : doi:10.1038/npre.2010.5442.1 : Posted 27 Dec 2010

Figure 8.

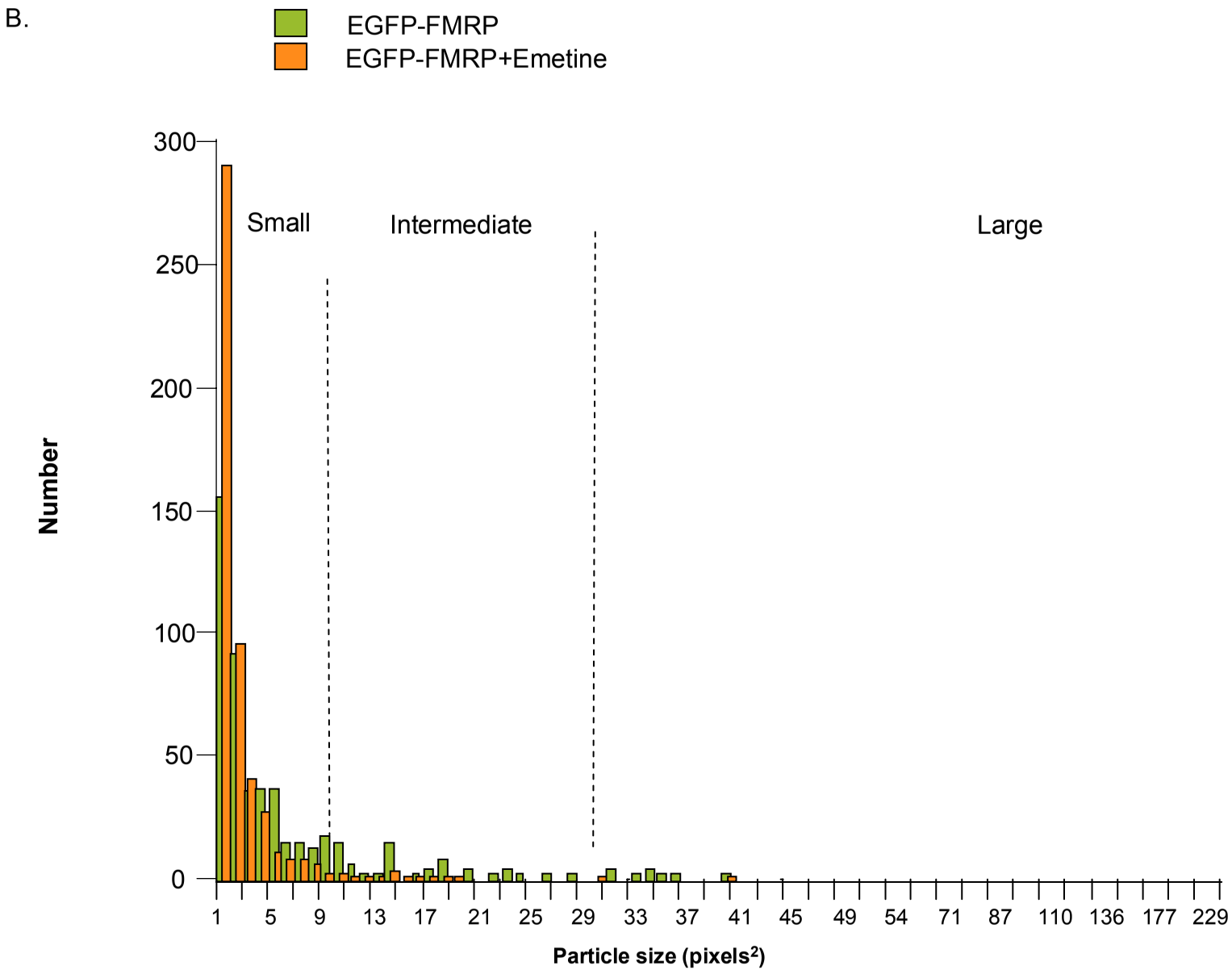

Figure 8.

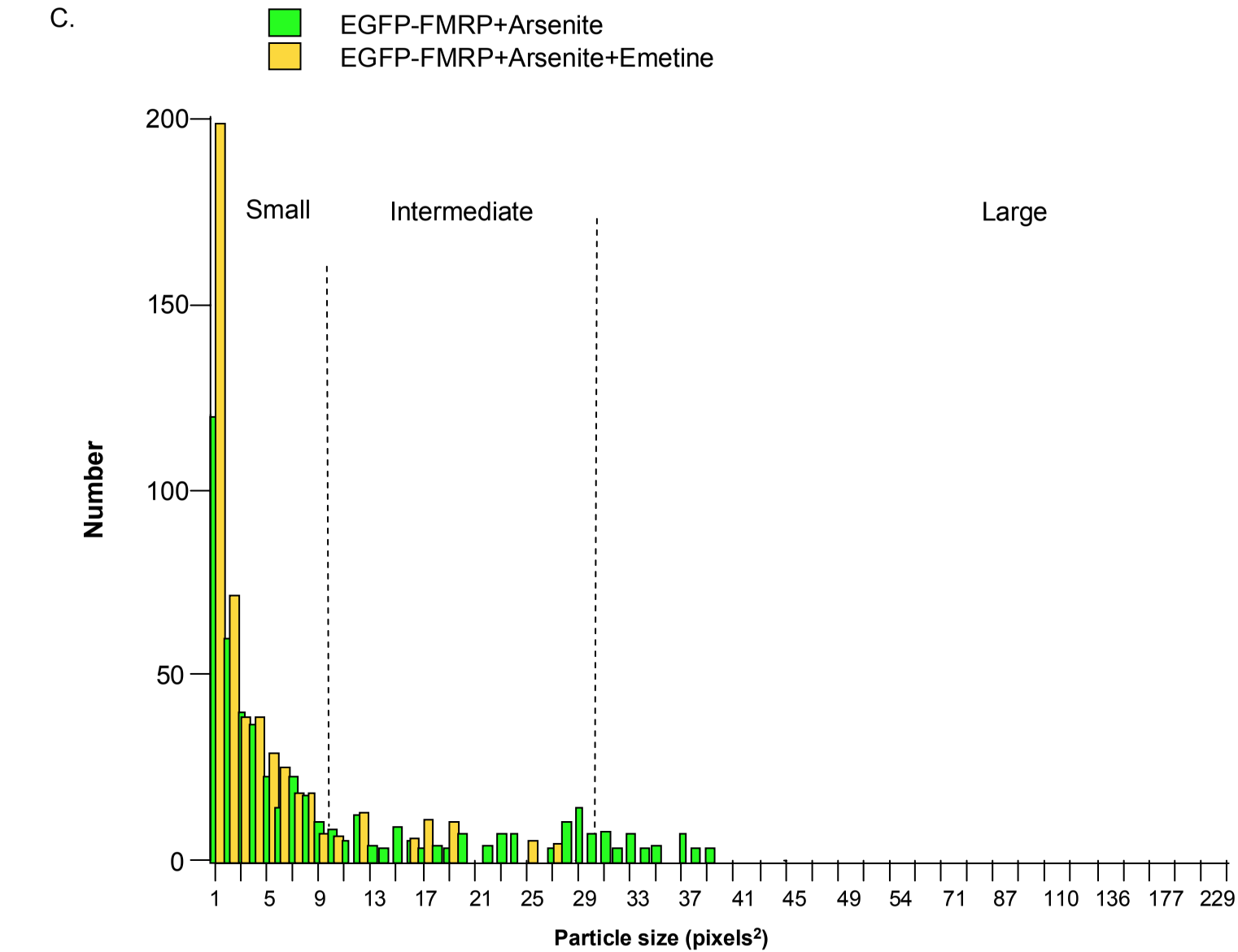

Figure 9.

A.

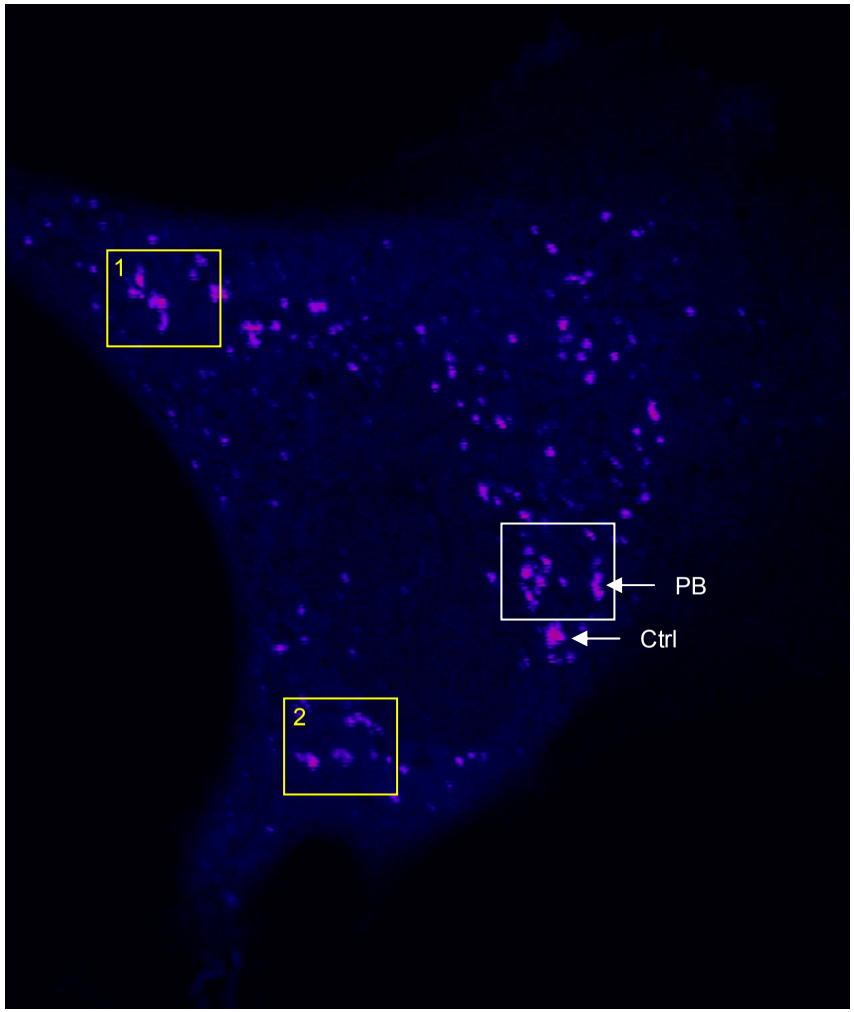
1
2
PB
Ctrl

B.

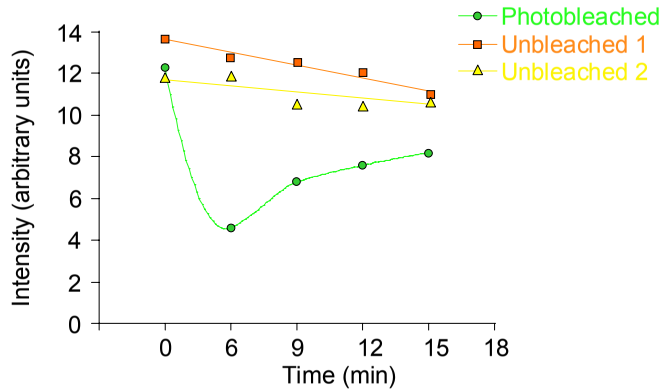
Photobleached
Unbleached 1
Unbleached 2
Intensity (arbitrary units)
Time (min)
0
2
4
6
8
10
12
14
0
6
9
12
15
18

C.

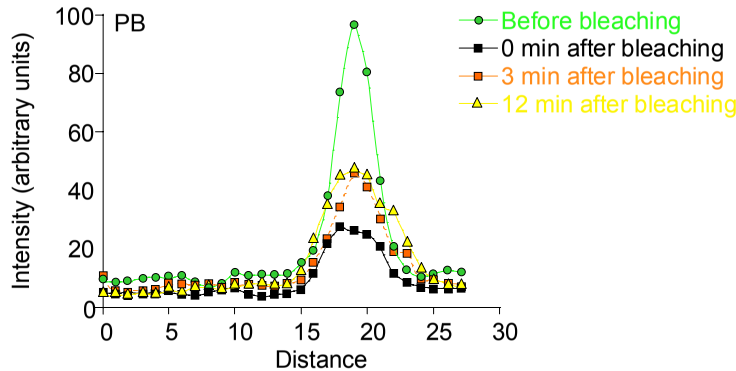
PB
Before bleaching
0 min after bleaching
3 min after bleaching
12 min after bleaching
Intensity (arbitrary units)
Distance
0
20
40
60
80
100
0
5
10
15
20
25
30

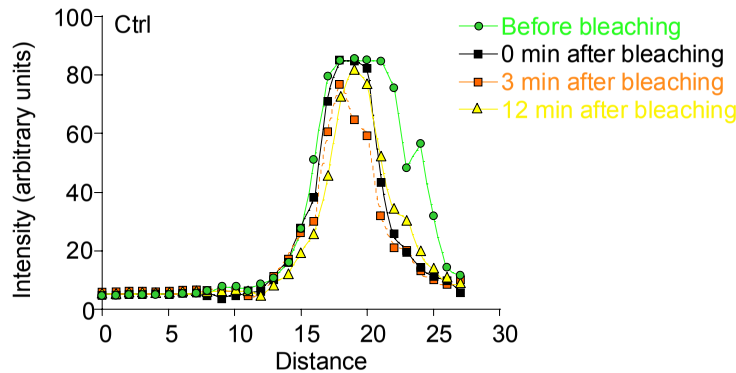
Ctrl
Before bleaching
0 min after bleaching
3 min after bleaching
12 min after bleaching
Intensity (arbitrary units)
Distance
0
20
40
60
80
100
0
5
10
15
20
25
30

Nature Precedings : doi:10.1038/npre.2010.5442.1 : Posted 27 Dec 2010

Figure 9.

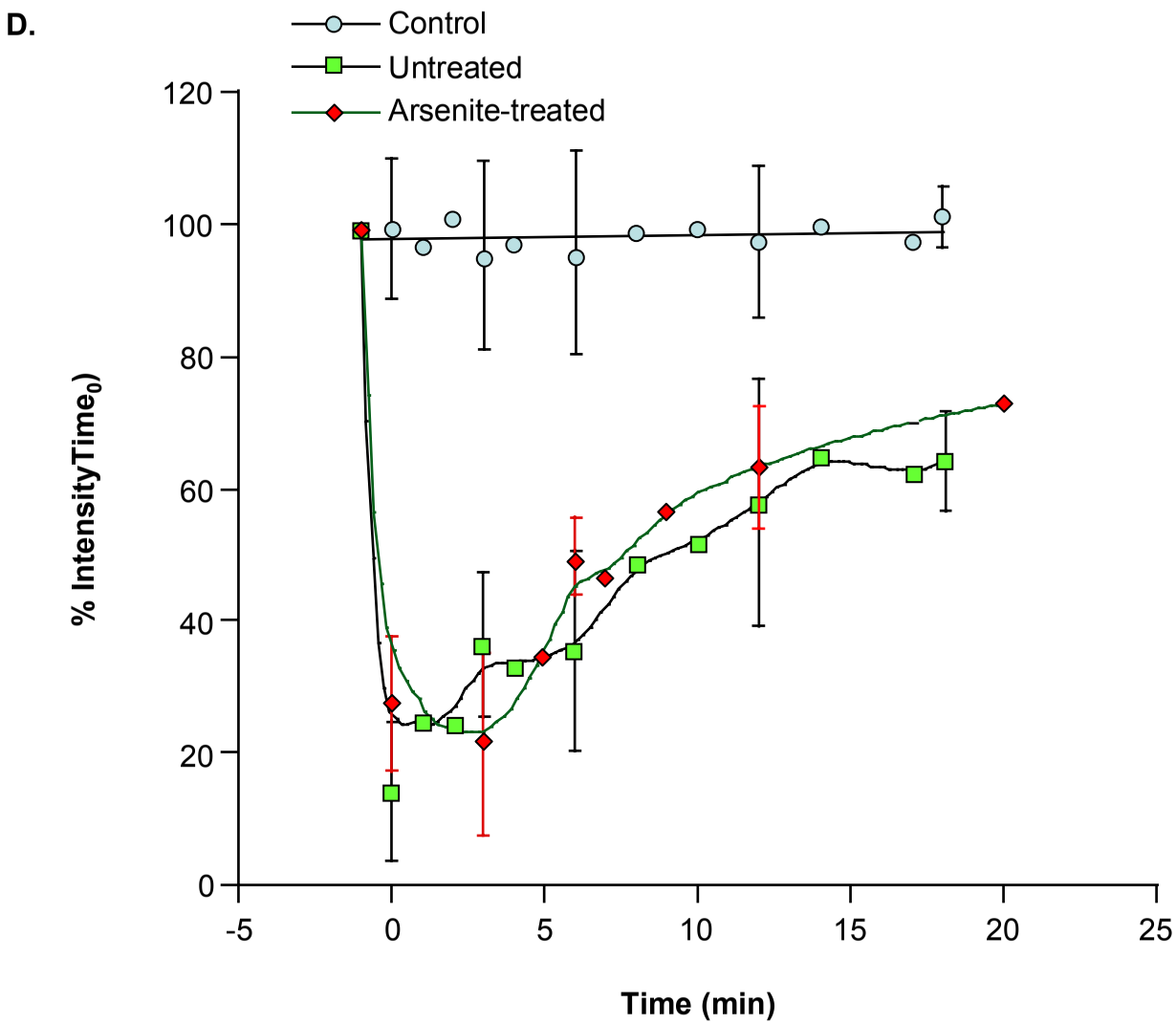

Figure 10A.

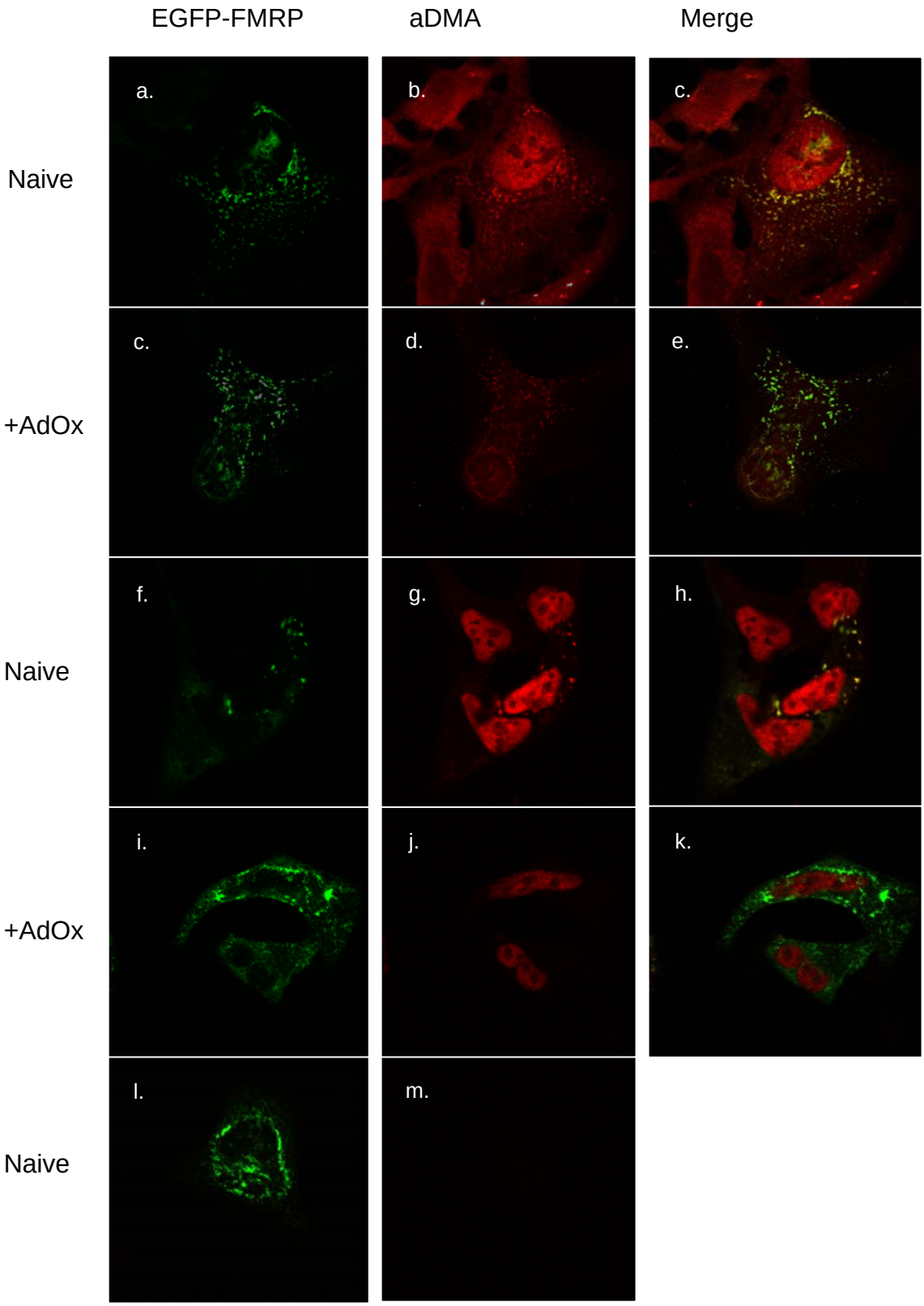

Figure 10B.

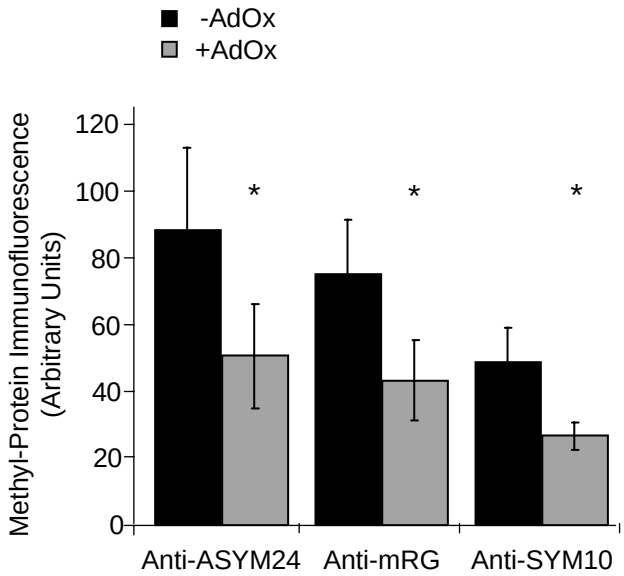

Figure 11A.

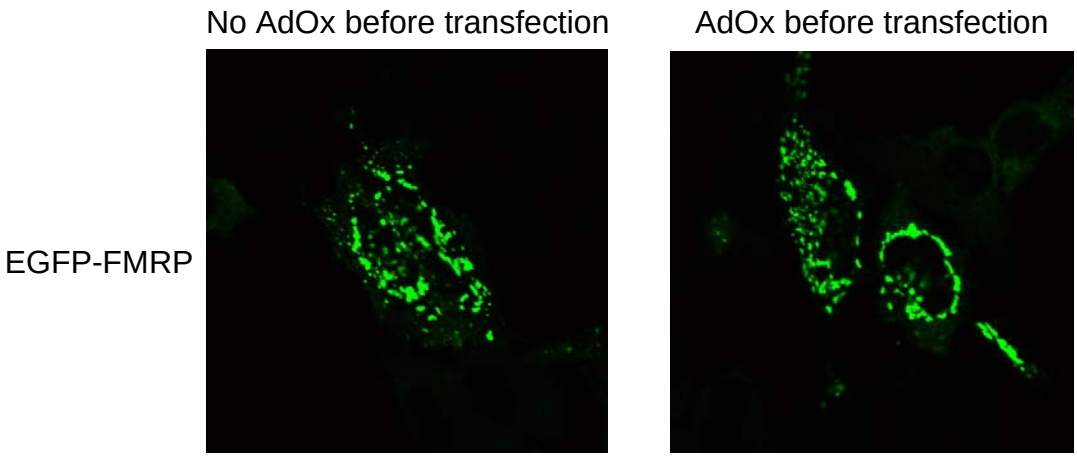

Nature Precedings : doi:10.1038/npre.2010.5442.1 : Posted 27 Dec 2010

Figure 11B.

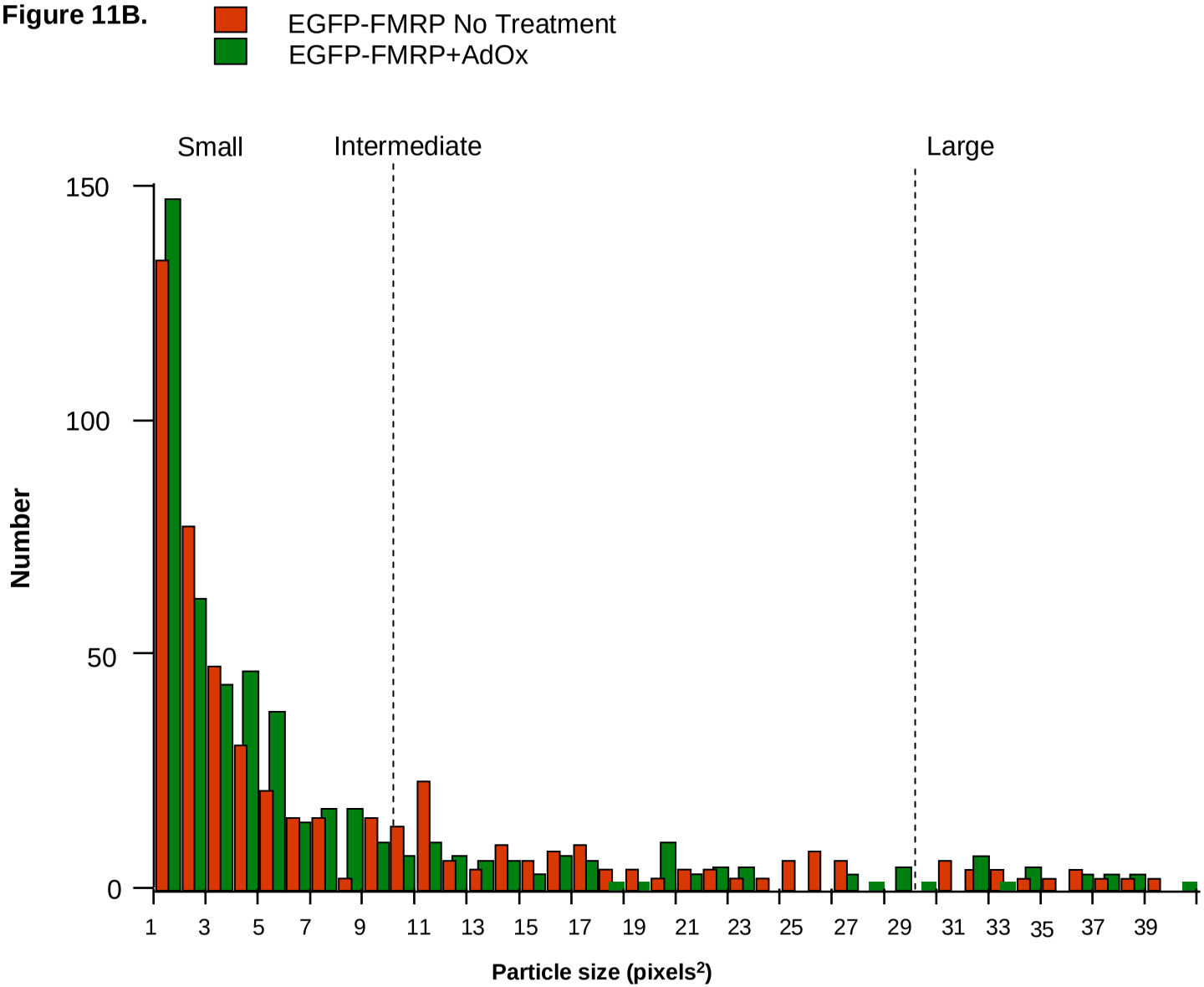

Figure 12A.

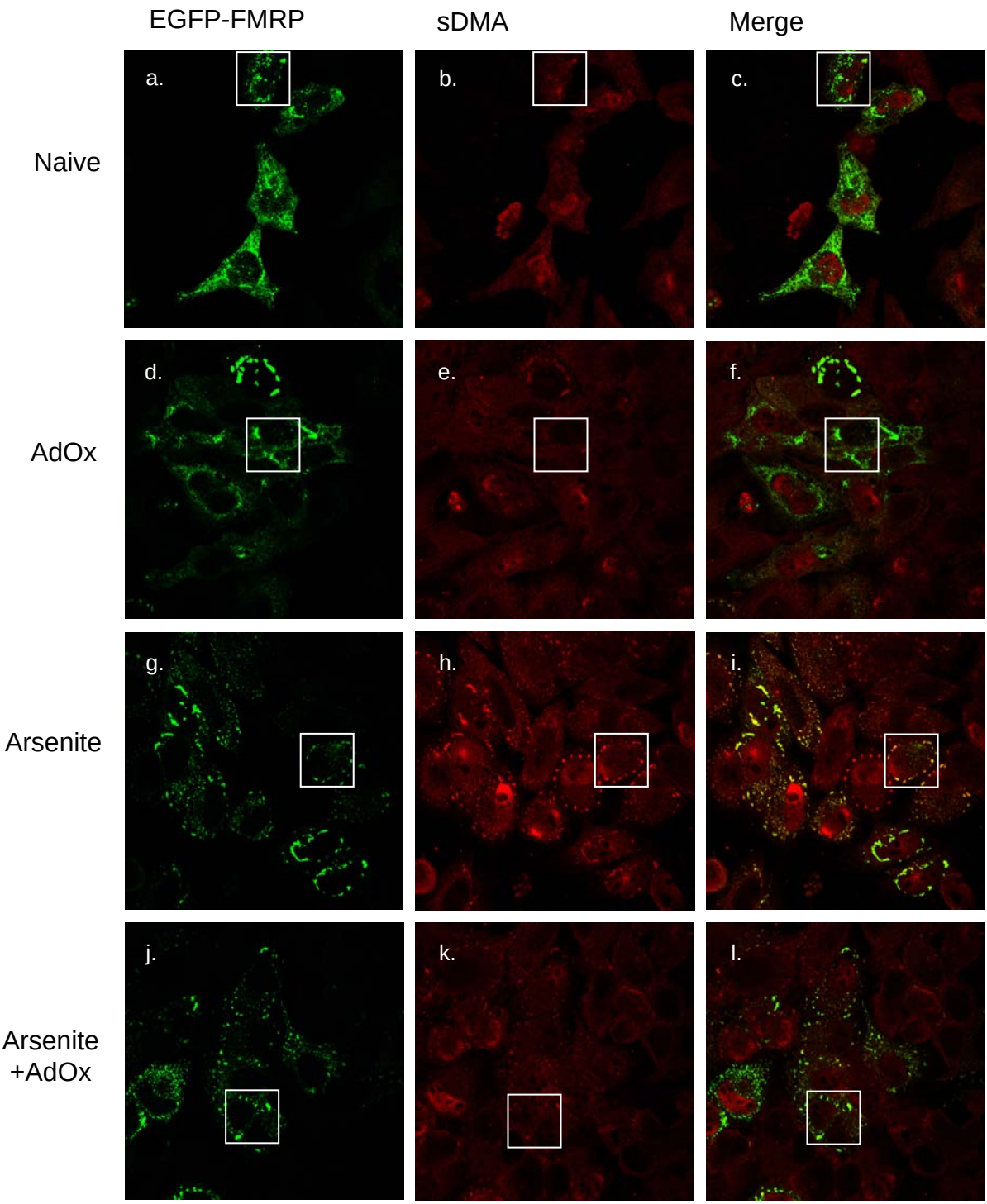

Figure 12B.

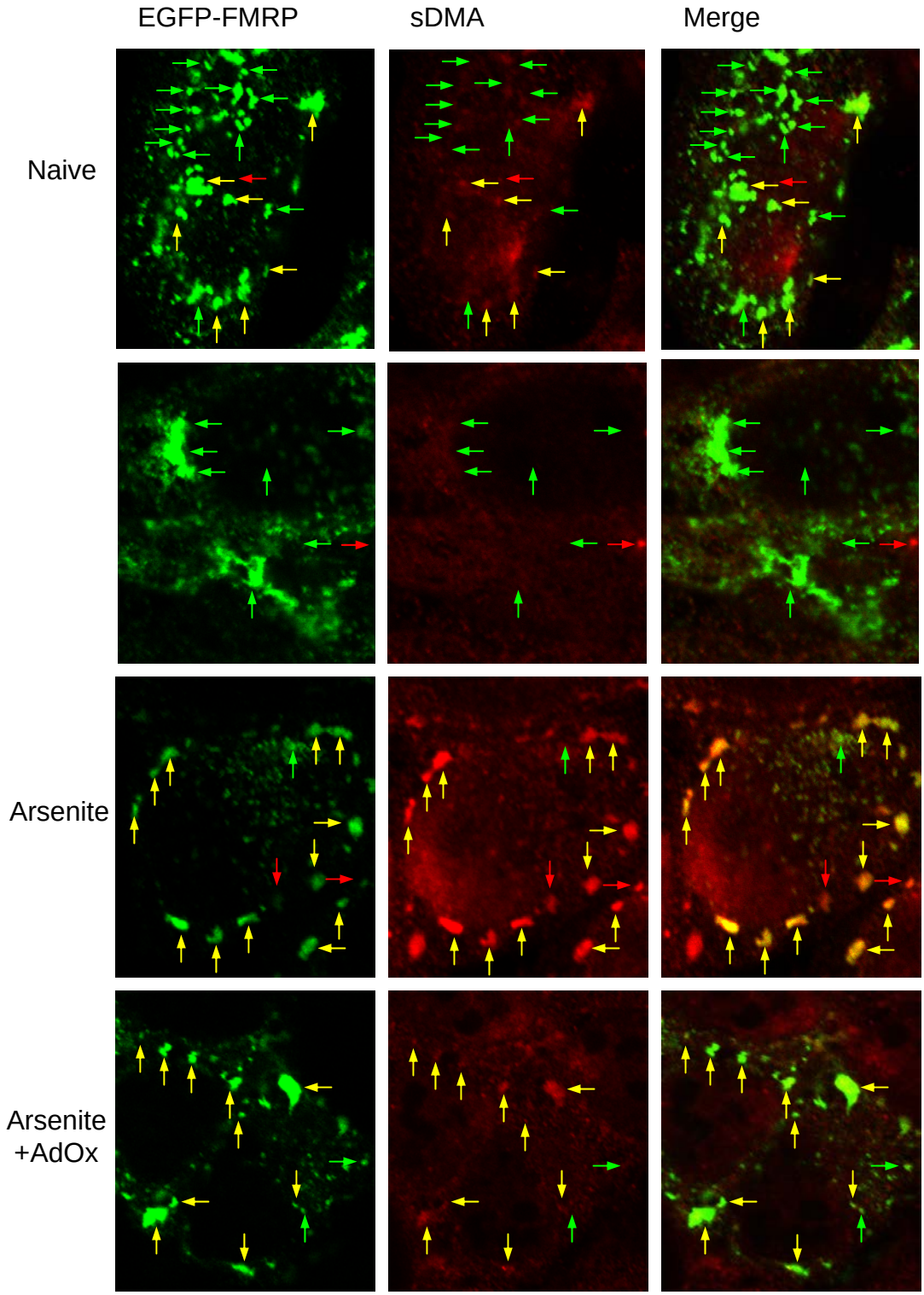

Figure 13.

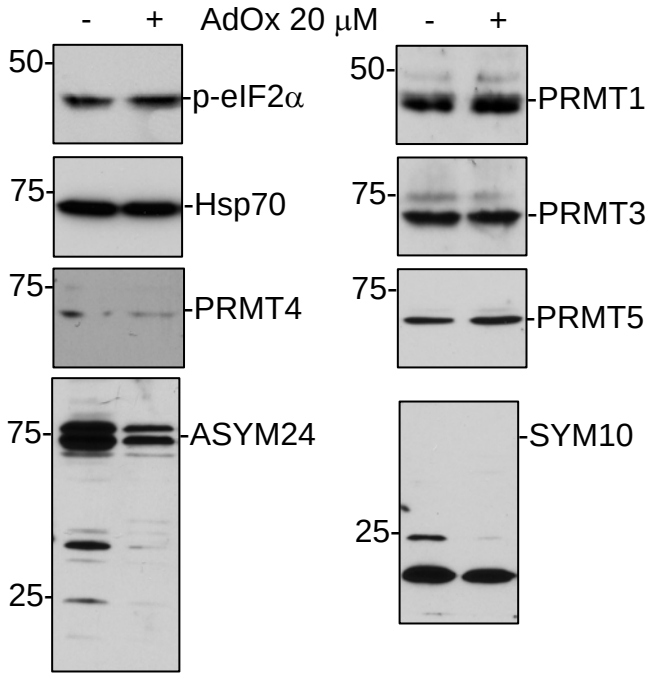

Figure 14.

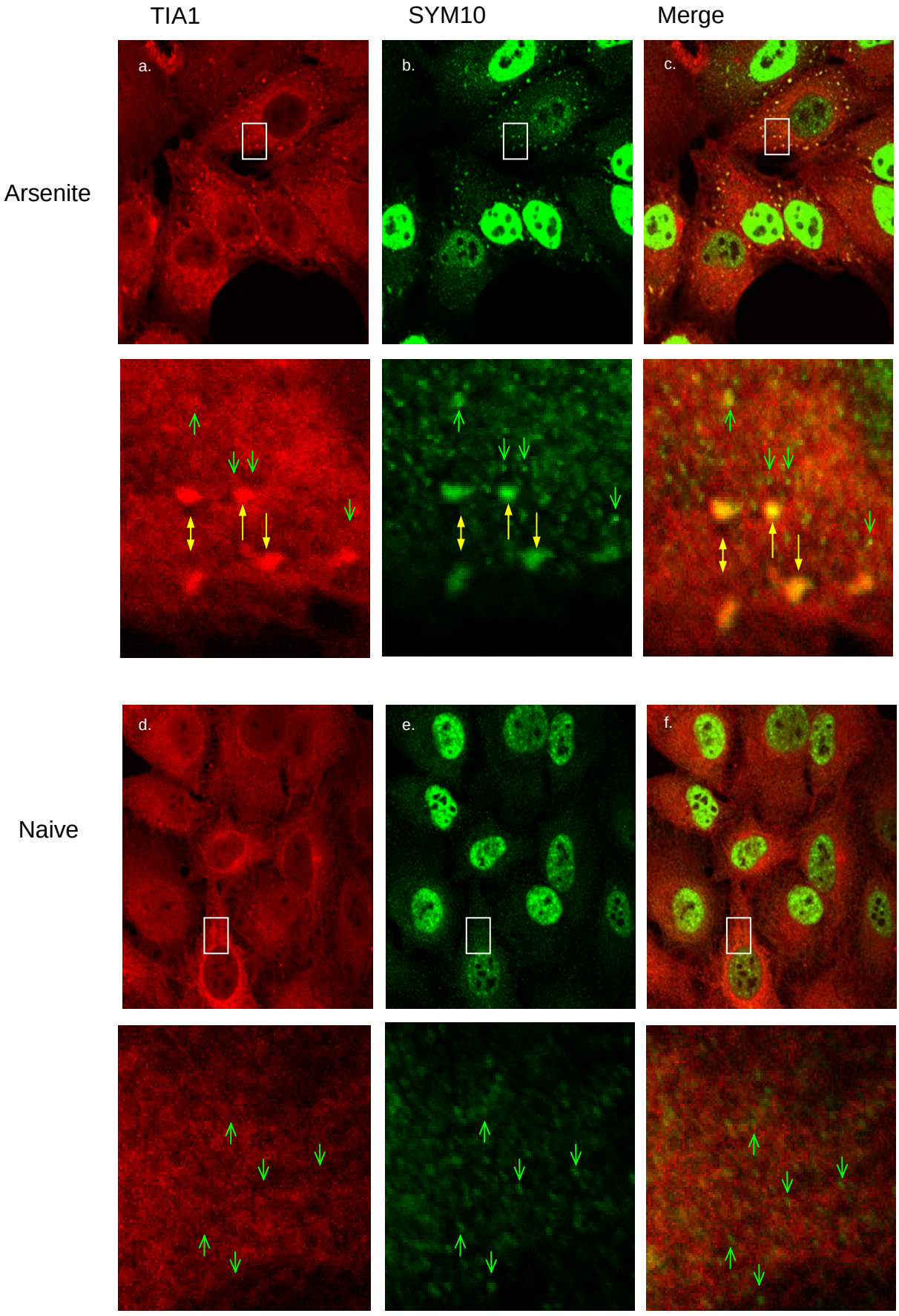

Figure 15A.

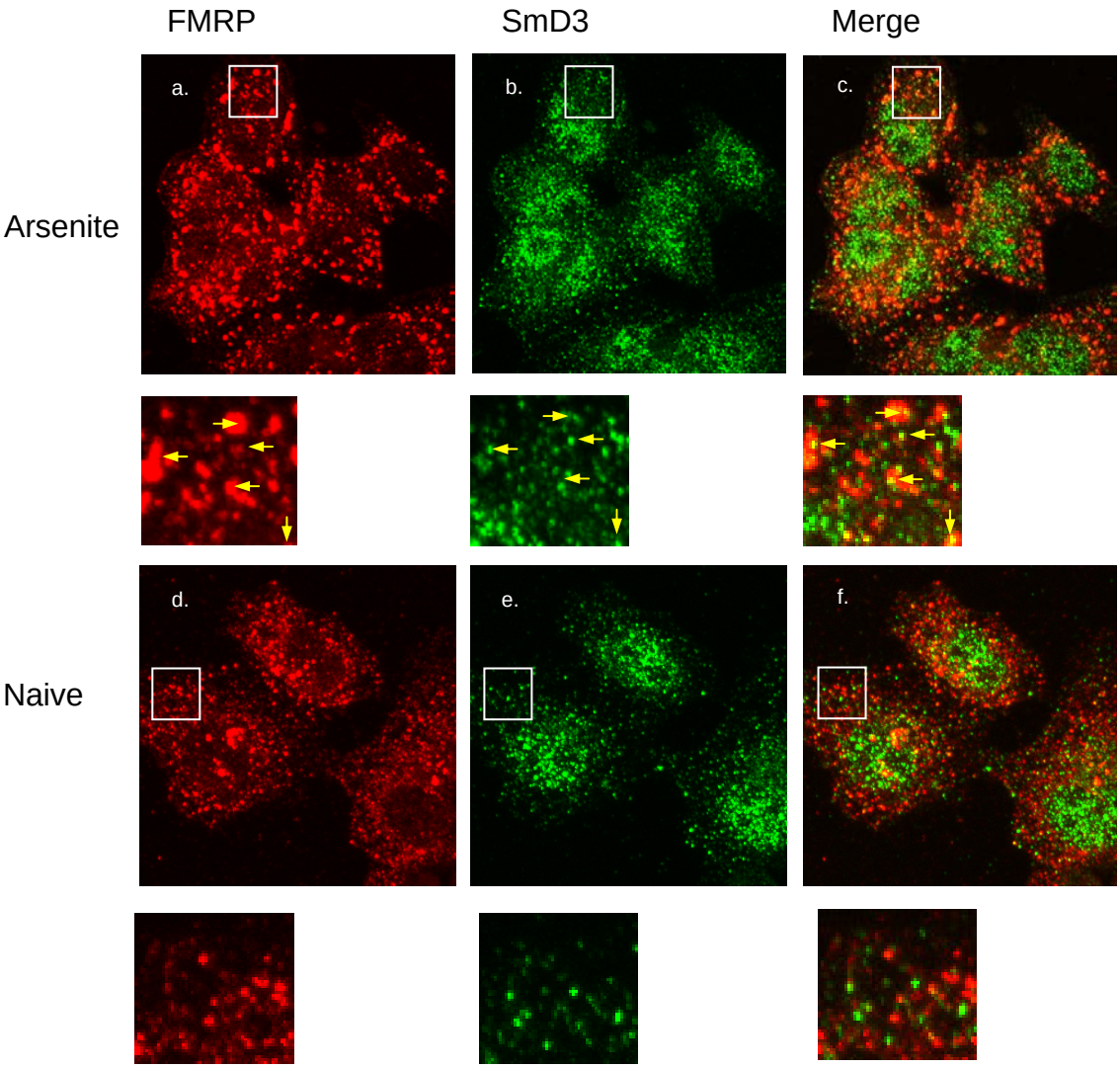

Figure 15B.

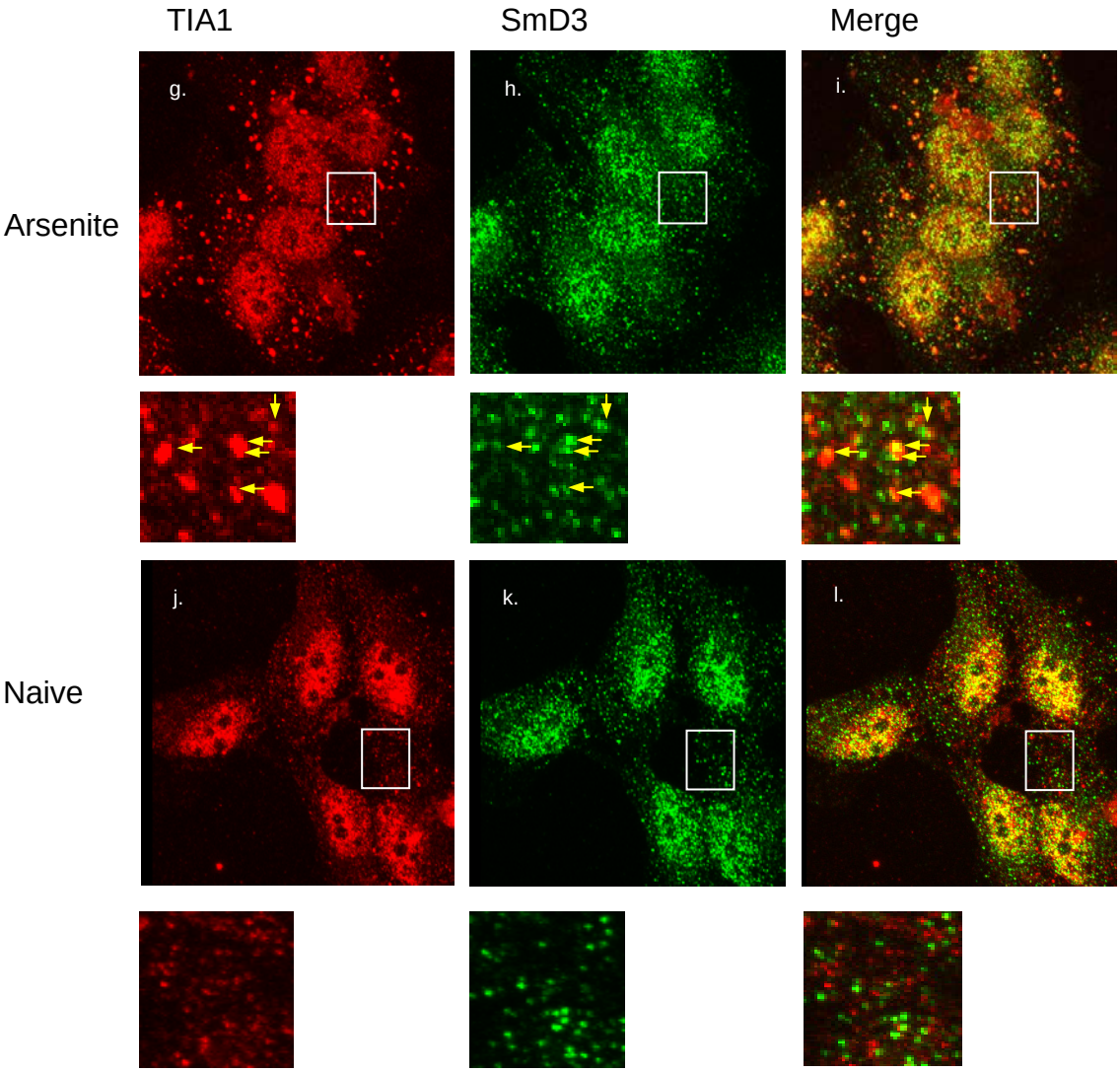

Figure 15C.

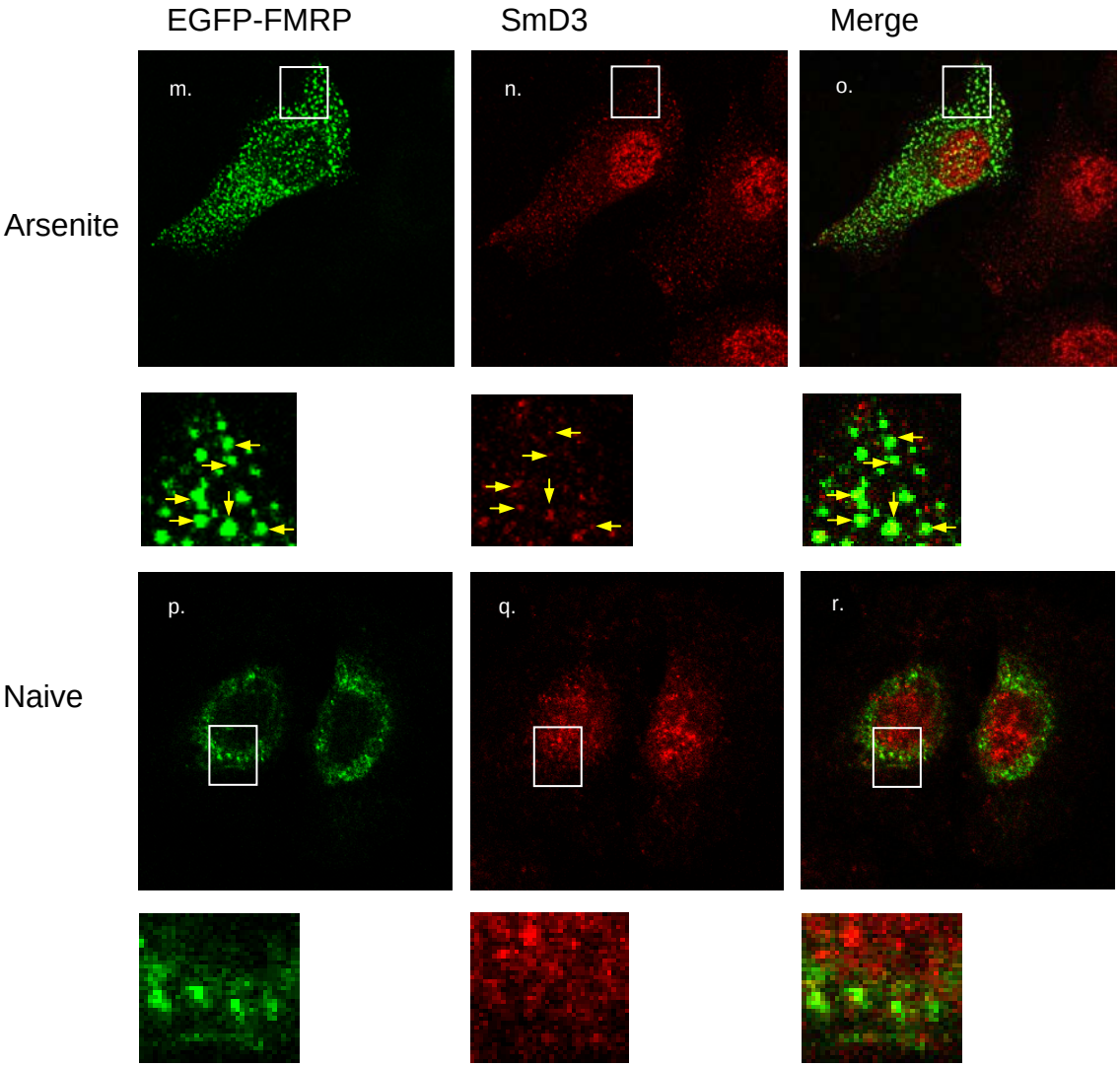

Figure 16A.

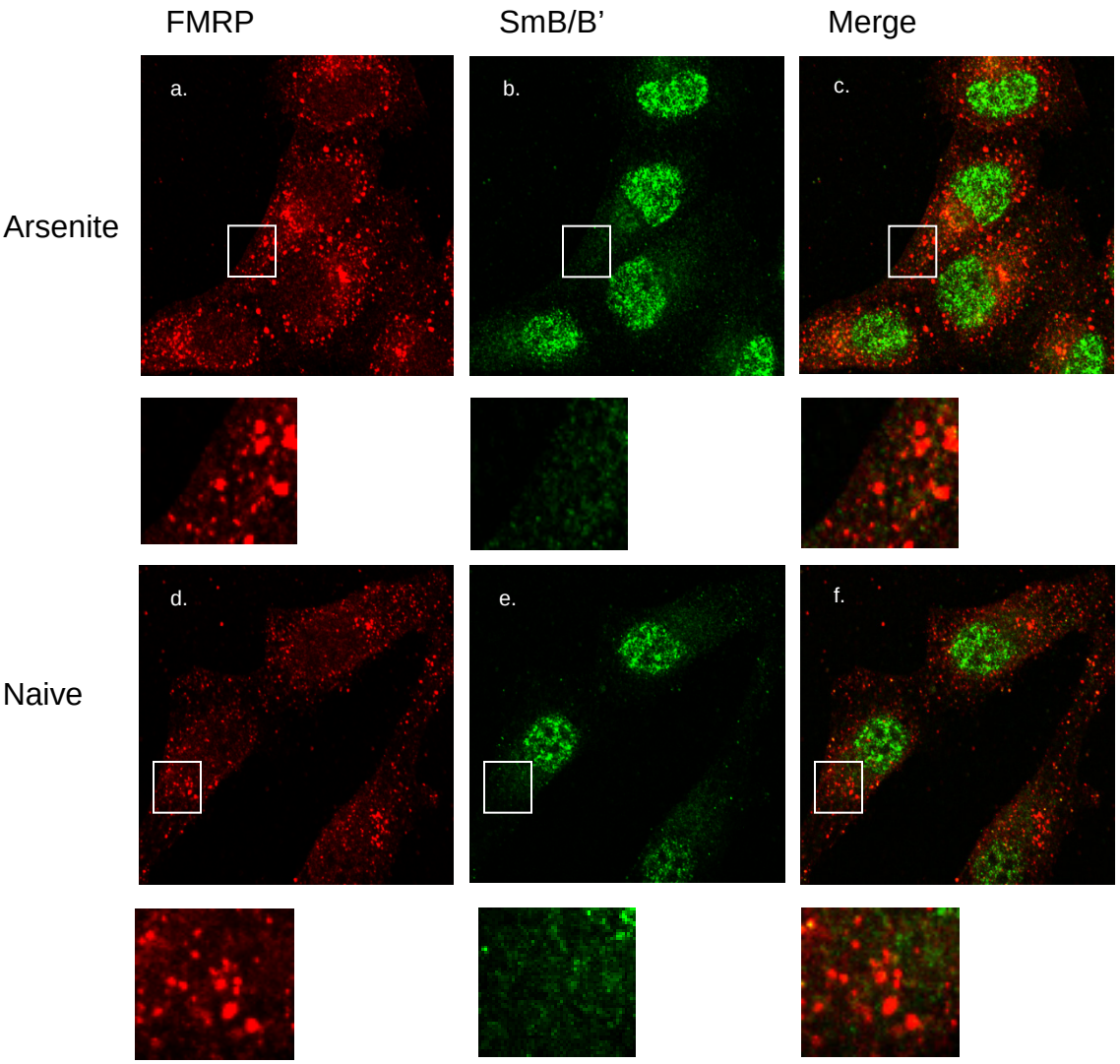

Figure 16B.

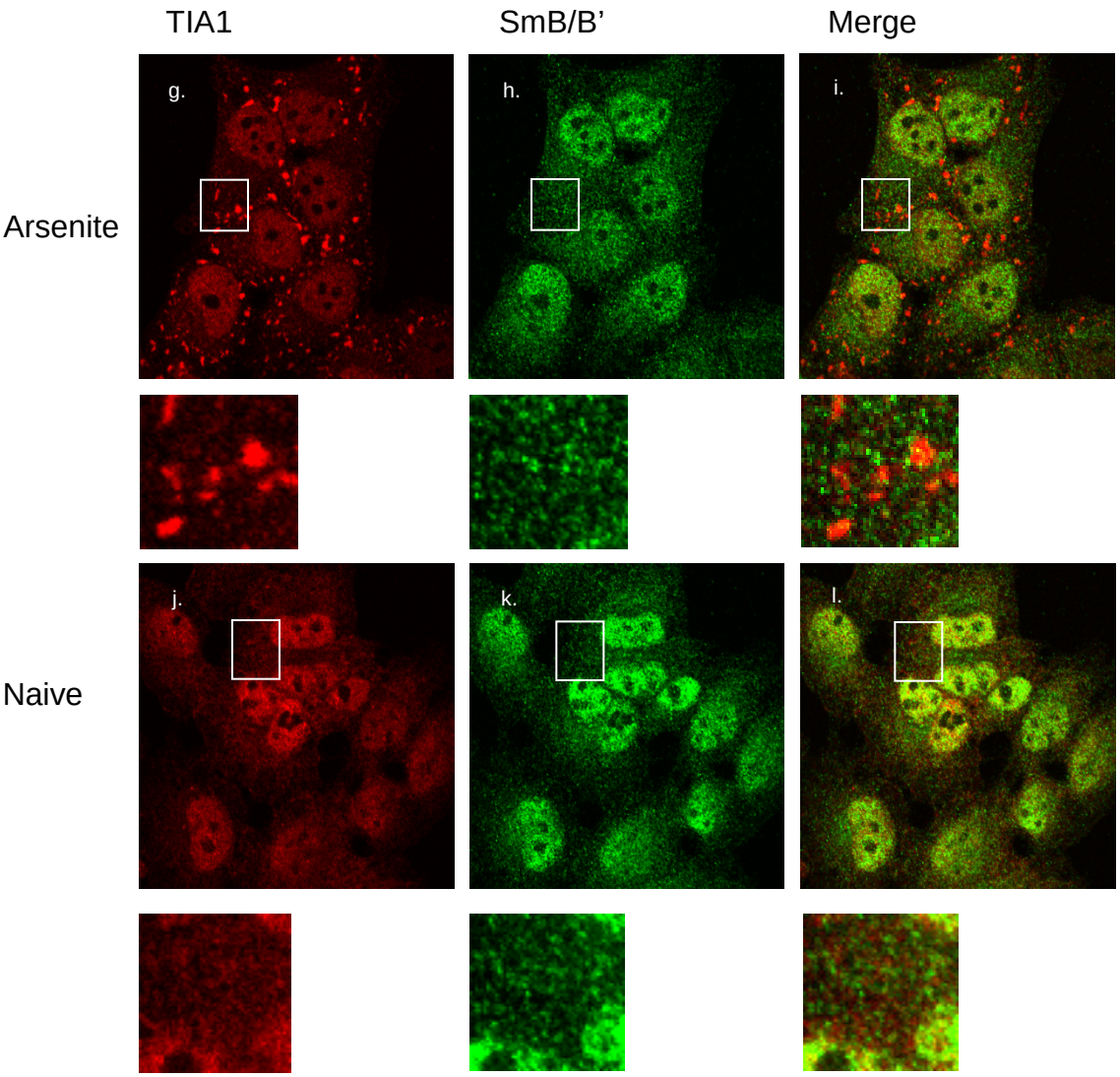

Figure 16C.

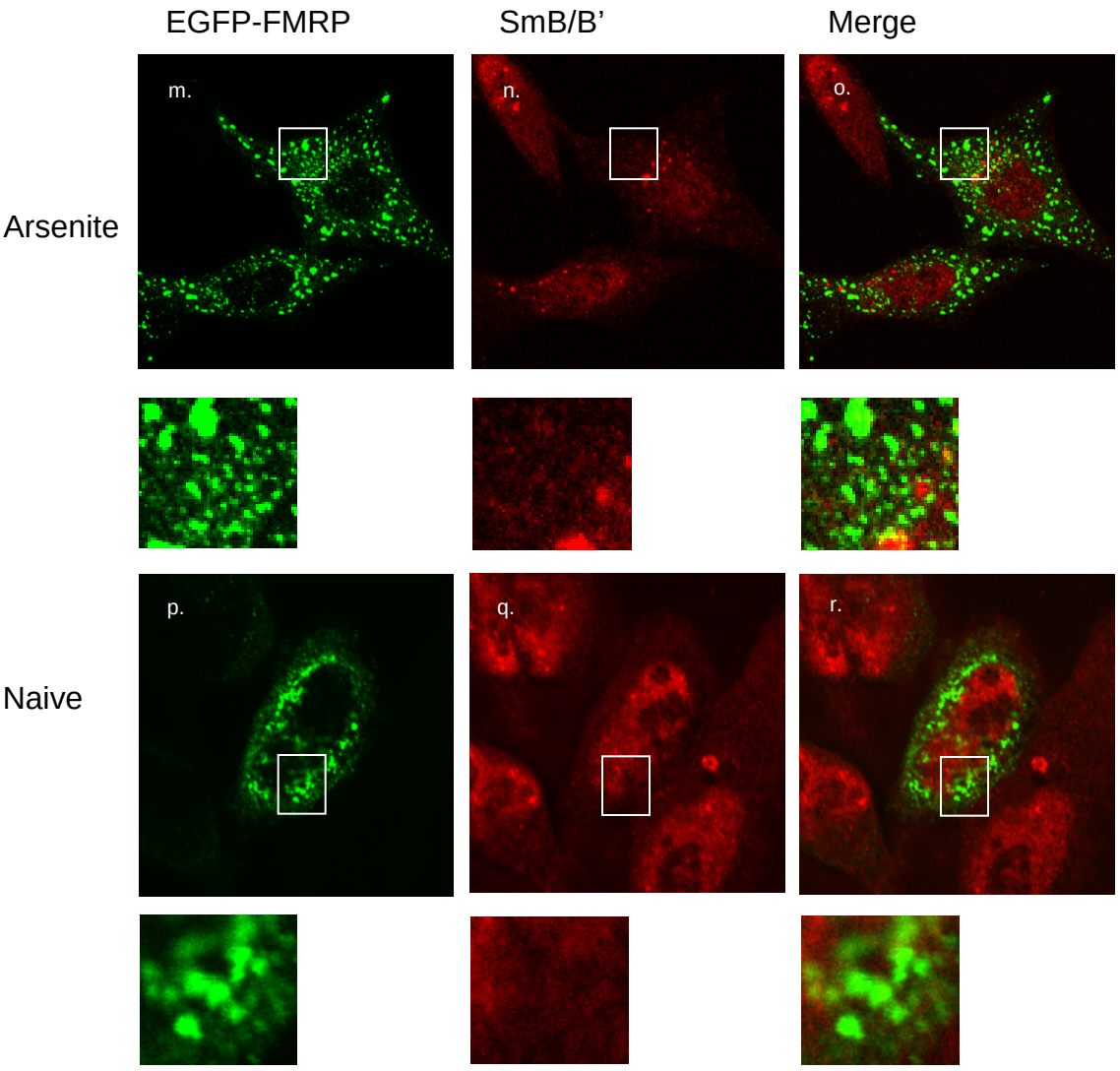

Figure 17.